ADVANCED MATERIALS

Supporting Information

for *Adv. Mater.*, DOI: 10.1002/adma.202001172

A Tumor-Microenvironment-Responsive Lanthanide–Cyanine FRET Sensor for NIR-II Luminescence-Lifetime In Situ Imaging of Hepatocellular Carcinoma

*Mengyao Zhao, Benhao Li, Yifan Wu, Haisheng He, Xinyan Zhu, Hongxin Zhang, Chaoran Dou, Lishuai Feng, Yong Fan, and Fan Zhang**

A Tumor-Microenvironment-Responsive Lanthanide–Cyanine FRET Sensor for NIR-II Luminescence-Lifetime In Situ Imaging of Hepatocellular Carcinoma

*Mengyao Zhao, Benhao Li, Yifan Wu, Haisheng He, Xinyan Zhu, Hongxin Zhang, Chaoran Dou, Lishuai Feng, Yong Fan, and Fan Zhang**

M. Zhao, B. Li, Y. Wu, H. He, X. Zhu, H. Zhang, Prof. Y. Fan and Prof. F. Zhang
Department of Chemistry, Shanghai Key Laboratory of Molecular Catalysis and Innovative Materials, State Key Laboratory of Molecular Engineering of Polymers and i*Chem*, Fudan University, Shanghai 200433, P. R. China.
E-mail: zhang_fan@fudan.edu.cn

C. Dou, and L. Feng
Shanghai Jiao Tong University Affiliated Sixth People's Hospital, Shanghai 200233, China.

Part A: Supplementary Experimental Section

Materials

Yttrium (III) chloride hexahydrate (99.9%), neodymium (III) chloride hexahydrate (99.9%), sodium trifluoroacetate (Na-TFA, 98%), 1-octadecene (ODE, 90%), oleic acid (OA, 90%), nitrosyl tetrafluoroborate ($NOBF_4$, 95%) and were purchased from Sigma-Aldrich. 6-aminohexanoic acid (99%) were purchased from Energy Chemical. N-(3-Dimethylaminopropyl)-N'-ethylcarbodiimide hydrochloride (EDC·HCl, 98.5%) and N-Hydroxysuccinimide (NHS, 98%) were purchased from Macklin Inc. COOH-PEG_{5000}-OCH_3 and COOH-PEG_{5000}-Mal were purchased from Ponsure Biotechnology. Sodium hydroxide (NaOH, 96%), ammonium fluoride (NH_4F, 96%), methanol (≥ 99.7%), ethanol (≥ 99.7%), isopropanol (≥ 99.7%) and N,N-dimethylformamide (DMF, ≥99.5%) were obtained from China National Pharmaceutical Group Corporation. Dulbecco's modified eagle medium (DMEM) cell culture was purchased from Gibco. Fetal bovine serum (FBS) was purchased from Excel. Trypsin (0.25%) and penicillin-streptomycin solution (100X) were purchased from MesGen Biotechnology. Glypiean-3 (GPC-3) antibody was purchased from Abcam. Other regents were purchased from Aladdin. All chemicals were used as received without any further purification.

Fabrication of β-$NaYF_4$@$NaYF_4$: 1%Nd core-shell nanoparticles

Fabrication of β-$NaYF_4$ core nanoparticles. Hexagonal phase (β-) $NaYF_4$ nanocrystals were fabricated following a previously reported thermolysis method[1]. In a typical procedure, $YCl_3·6H_2O$ (0.99 mmol), $NdCl_3·6H_2O$ (0.01 mmol), OA (6.0 mL) and ODE (15.0 mL) were mixed together and heated to 140 °C under vacuum until a clear solution formed, after that, the solution was cooled down to room temperature. A methanol solution (10.0 mL) of ammonium fluoride (4 mmol) and sodium hydroxide (2.5 mmol) was added and stirred for 1 h. The reaction mixture was then heated to 60 °C and maintained for 0.5 h to remove the methanol. Afterward, the solution was heated to 300 °C (~ 10 °C min^{-1}) and maintained for 90 min under a gentle argon flow. Then, the solution was cool down to room temperature and the nanoparticle products were centrifuged and washed twice with ethanol. The nanoparticles were finally dispersed in 10 mL of cyclohexane for further use.

Preparation of shell precursors

Y:1%Nd-OA (0.10 M) host precursor.

A mixture of $YCl_3 \cdot 6H_2O$ (4.95 mmol), $NdCl_3 \cdot 6H_2O$ (0.05 mmol), OA (20.0 mL), and ODE (30.0 mL) was loaded in a reaction container and heated at 140 °C under vacuum with magnetic stirring for 30 min to remove residual water and oxygen. Then the colorless Y:1%Nd-OA precursor solution (0.10 M) was obtained.

Na-TFA-OA (0.40 M) precursor.

A mixture of Na-TFA (4.00 mmol) and OA (10.0 mL) was loaded in a container at room temperature under vacuum with magnetic stirring to remove residual water and oxygen. Then the colorless Na-TFA-OA precursor solution (0.40 M) was obtained.

Fabrication of β-$NaYF_4$@$NaYF_4$:1%Nd core-shell nanoparticles.

The core-shell nanoparticles were fabricated by using the one-pot successive layer-by-layer (SLBL) protocol, which was developed by our group.[2] 5 mL of the purified $NaYF_4$ core nanoparticles solution (~ 0.5 mmol) were mixed with 4.0 mL of OA and 6.0 mL of ODE. The flask was pumped down at 70 °C for 30 min to remove cyclohexane, along with any residual air. Subsequently, the system was switched to Ar flow and the reaction mixture was further heated to 260 °C at a rate of ~ 20 °C min^{-1}. Then pairs of Y:1%Nd -OA (0.10 M, 1.0 mL) and Na-TFA-OA (0.40 M, 0.50 mL) precursors were alternately introduced by dropwise addition at 280 °C and the time interval between each injection was 15 min. Finally, the obtained $NaYF_4$@$NaYF_4$:1%Nd core-shell nanoparticles were precipitated and washed in the same way as the core nanoparticles and dispersed in cyclohexane.

Synthesis of MY-dyes

Procedure for synthesis of dye MY-1005.

1-ethyl-2-phenyl-1H-indole (compound **1**, 4.3 mmol, 950 mg) and acetyl chloride (2.2 mmol) in acetic anhydride (20 mL) was heated at 55 ^oC for 4h. N-[(3-(Anilinomethylene)-2-chloro-1-cyclopenten-1-yl) methylene] aniline monohydrochloride (compound **2,** 1.1 mmol, 344 mg) and potassium tetrafluoroborate (1.1 mmol, 125.9 mg) were added to mixed solution, and then heated at 100 ^oC for 2 h. After cooling, the solution was treated with water (100 mL). The precipitate was filtered and recrystallized in EtOH to give **MY-1005** (921 mg, 75%).

^{1}H NMR (400 MHz, DMSO-d_6) δ 8.32-8.30(d, 2H), 7.60-7.59 (m, 10H), 7.56-7.54(m, 6H), 7.46-7.40(m, 4H), 7.31-7.22(m, 10H), 7.17-7.15(m, 2H), 7.12-7.10(m, 2H), 7.07-7.05(m, 2H), 6.92-6.89 (t, 2H), 3.97-3.92(m, 8H), 1.78(s, 4H), 1.15-1.11(t, 12H).^{13}C NMR (101 MHz, DMSO-d_6) δ 146.78, 135.70, 132.40, 131.10, 130.88, 130.42, 130.08, 129.69, 129.52, 128.42, 127.93, 127.02, 123.76, 122.97, 122.66, 115.68, 111.23, 39.22, 30.47, 15.65.

HRMS (+ESI) $[C_{75}H_{64}ClN_4]^{2-}$: calculated: 1055.4814, measured: 1055.4800.

Procedure for synthesis of dye MY-1058.

Synthesis of compounds 4.

2-Phenylindole (compound **3**, 2.0 mmol, 386 mg) and Sodium hydride (60%, 2.1 mmol, 84 mg) were mixed in anhydrous tetrahydrofuran (15 mL) and stirred at 0 ^{o}C for 30 min. To this solution was added butanesultone (2.0 mmol, 272 mg) and then heated at 100 °C for 2 h. After cooling, the solution was treated with isopropyl alcohol. The white solid was collected by filtration to afford compounds **4** (667 mg, 95%).

Compound **4**: ^{1}H NMR (400 MHz, DMSO-d_6) δ 7.56-7.52 (m, 6H), 7.47-7.45 (m, 1H), 7.19-7.15 (m, 1H), 7.09-7.04(m, 1H), 6.54 (s, 1H), 4.19-4.15 (t, 2H), 2.34-2.28 (m, 2H), 1.67-1.64 (m, 2H), 1.46-1.42 (m, 2H).^{13}C NMR (101 MHz, DMSO-d_6) δ 141.2, 137.7, 133.1, 129.5, 129.2, 128.5, 128.1, 121.8, 120.6, 120.0, 111.0, 102.2, 51.1, 43.8, 29.3, 22.9.

Synthesis of dyes MY-1058.

Compound **4** (4.3 mmol, 1.14 g) and acetyl chloride (2.2 mmol, 172 mg) in acetic anhydride (20 mL) was heated at 55 °C for 4h. N-[(3-(Anilinomethylene)-2-chloro-1-cyclopenten-1-yl) methylene] aniline monohydrochloride (compound **2,** 1.1 mmol, 340 mg) was added to mixed solution, and then heated at 100 °C for 2 h. After cooling, the solution was treated with ether (60 mL). The precipitate was collected by filtration. The product was purified by preparative RP HPLC (Waters C18 (5 μm, 250 mm × 20 mm) to give **MY-1058** (1068 mg, 64%).

^{1}H NMR (400 MHz, DMSO-d_6) δ 7.71-7.69 (d, 4H), 7.36-7.24 (m, 26H), 7.10-7.06 (d, 4H), 6.83-6.79 (d, 2H), 6.16-6.13 (d, 2H), 4.12 (m, 8H), 2.32-2.28 (m, 8H), 1.82 (s, 4H), 1.67-1.64 (m, 8H), 1.46-1.45 (m, 8H).^{13}C NMR (101 MHz, DMSO-d_6) δ 151.4, 148.5, 142.4, 137.7, 137.6, 137.6, 130.8, 128.9, 128.7, 124.1, 124.0, 123.8, 120.6, 120.5, 112.4, 112.2, 112.1, 51.1, 44.5, 29.0, 25.8, 22.9.

HRMS (-ESI) $[C_{83}H_{76}ClN_4O_{12}S_4Na]^{2-}$: calculated: 753.1970, measured: 753.1981, $[C_{83}H_{76}ClN_4O_{12}S_4]^{3-}$:

calculated: 494.4683, measured: 494.4689.

Procedure for synthesis of dyes MY-1057.

Synthesis of compounds 5.

2-Phenylindole (compound **3**, 3.0 mmol, 579 mg), ethyl 5-bromovalerate (6.0 mmol, 1.254 g) and cesium carbonate (6.0 mmol, 1.95 g) were mixed in anhydrous N,N-Dimethylformamide (20 mL) and stirred at 0 °C for 10 h. Water (60 mL) was added and the mixture was extracted with EtOAc. The organic layer was washed sequentially with water and saturated brine, dried over anhydrous sodium sulfate, and concentrated. The residue was purified by column chromatography on silica gel to afford compounds **5** (713 mg, 74%).

^{1}H NMR (400 MHz, $CDCl_3$) δ 7.67-7.65 (d, 1H), 7.50-7.38 (m, 6H), 7.27-7.23 (m, 1H), 7.17-7.15 (m, 1H), 6.54 (s, 1H), 4.21-4.11 (t, 2 H), 4.14-4.06 (m, 2H), 2.19-2.15 (m, 2H), 1.76-1.72 (m, 2H), 1.51-1.47 (m, 2H), 1.24-1.21 (m, 3H). ^{13}C NMR (101 MHz, DMSO-d_6) δ 173.36, 141.52, 137.49, 133.38, 129.67, 128.77, 128.47, 128.23, 121.82, 120.85, 120.07, 110.20, 102.48, 60.54, 43.75, 33.89, 29.57, 22.36, 14.45.

Synthesis of compounds 6.

A 2.5 mol/L aqueous solution of sodium hydroxide (1.0 mL) was added to a mixture of compound **5** (1.0 mmol, 321 mg) and EtOH (10 mL), and the mixture was stirred for 4 h at 80 °C. The reaction mixture was acidified with 2 mol/L hydrochloric acid and extracted with EtOAc. The organic layer was washed sequentially with water and saturated brine, dried over anhydrous sodium sulfate, and concentrated. The residue was purified by column chromatography on silica gel to afford compounds **6** (246 mg, 84%).

^{1}H NMR (400 MHz, $CDCl_3$) δ 7.66-7.64 (d, 1H), 7.49-7.38 (m, 6H), 7.27-7.23 (m, 1H), 7.17-7.14 (m, 1H), 6.54 (s, 1H), 4.22-4.18 (t, 2 H), 2.23-2.19 (m, 2H), 1.77-1.73 (m, 2H), 1.50-1.46 (m, 2H). ^{13}C NMR (101 MHz, $CDCl_3$) δ 179.29, 141.50, 137.49, 133.33, 129.66, 128.79, 128.46, 128.27, 121.85, 120.88, 120.09, 110.15, 102.54, 43.61, 33.44, 29.42, 21.94.

Synthesis of dyes MY-1057.

Compound **6** (4.3 mmol, 1.26 g) and acetyl chloride (2.2 mmol, 172 mg) in acetic anhydride (20 mL) was heated at 55 °C for 4h. N-[(3-(Anilinomethylene)-2-chloro-1-cyclopenten-1-yl) methylene] aniline monohydrochloride (compound **2,** 1.1 mmol, 340 mg) was added to mixed solution, and then heated at

100 °C for 2 h. After cooling, the solution was treated with ether (60 mL). The precipitate was collected by filtration. The product was purified by preparative RP HPLC (Waters C18 (5 μm, 250 mm × 20 mm) to give **MY-1057** (779 mg, 54%).

^{1}H NMR (400 MHz, DMSO-d_6) δ 7.69-7.67 (d, 4H), 7.29-7.26 (m, 26H), 7.05-7.04 (m, 4H), 6.84-6.80 (d, 4H), 6.14-6.11 (d, 2H), 4.16 (m, 8H), 2.09-2.06 (m, 8H), 1.91 (s, 4H), 1.59-1.55 (m, 8H), 1.31-1.25 (m, 8H). ^{13}C NMR (101 MHz, DMSO-d_6) δ 174.50, 172.85, 153.63, 151.76, 147.10, 144.71, 142.53, 137.83, 137.03, 133.71, 131.27, 130.75, 130.07, 129.24, 128.89, 127.18, 124.44, 116.31, 111.96, 47.69, 33.42, 29.09, 21.97, 21.54.

HRMS (+ESI) $[C_{87}H_{80}ClN_4O_8]^+$: calculated: 1343.5659, measured: 1343.5651.

Fabrication of DSNP@MY-1005, DSNP@MY-1058 and DSNP@MY-1057-GPC-3.

Transferring hydrophobic $NaYF_4$@$NaYF_4$: 1%Nd downshifting nanoparticles (DSNPs) to hydrophilic DSNP-NH_2 nanoparticles.

The phase transfer method used in this work was similar to the method previously reported by Liang *et al.* [2] Typically, 1 mL of oleic acid capped UCNPs in cyclohexane (10 mg mL^{-1}) was mixed with 3 mL cyclohexane, 3 mL DMF and $NOBF_4$ (5.8 mg, 50 μmol) in a centrifuge tube. The centrifuge tube was vortexed vigorously for 10 min at room temperature and rested for 5 min. Then the supernatant cyclohexane was discarded and 3 mL isopropanol was added to the centrifuge tube. The BF_4^- modified DSNPs was centrifuged down (15000 rpm, 15 min) and dissolved in 0.5 mL DMF. The solution of DMF was mixed with a water solution (9 mL) of 6-aminohexanoic acid (0.262 g, 2 mmol) and stirred vigorously for 2 h. Excess 6-aminohexanoic acid was purified by centrifugation and washing with deionized water.

MY-dyes modification.

MY-dyes were loaded on the surface of DSNPs by hydrophobic interaction following the literature published before with some modifications[3]. Briefly, polymer COOH-PEG_{5000}-OCH_3 (100 mg) was dissolved in water (5 mL) containing EDC (47.9 mg, 0.25 mmol) and NHS (57.5 mg, 0.5 mmol) to form the active succinimidyl ester for 4 h. Then the mixture was added slowly to 5 mL DSNP-NH_2 (3 mg mL^{-1}) in water with 30 min sonication[4]. After vigorous magnetic stirring overnight, the products

were purified by centrifugation (15,000 rpm, 15 min) and re-dispersed in 500 μl dimethyl sulfoxide (DMSO). Then MY-dyes (0.3 μM) in DMSO were added to the DSNP-NH_2 solutions, then 10 ml water was added under sonication for 30 min. Finally, DSNP@MY-dyes was collected by centrifugation (15,000 rpm, 15 min) followed by several times washing to remove excess reactant.

GPC-3 antibody conjugation.

To conjugate GPC-3 antibody, COOH-PEG_{5000}-OCH_3 (90 mg) and COOH-PEG_{5000}-Mal (10 mg) were used in MY-dyes modification section instead of COOH-PEG_{5000}-OCH_3 (100 mg). Next 10 μl of the antibodies at a concentration of ~1 mg ml^{-1} were reduced with 10 mM of tris (2-carboxyethyl) phosphine (TCEP) by shaking for 1 h to expose free sulfhydryls. The reduced antibodies were mixed with the maleimide-conjugated nanoparticles. Finally, the conjugated nanoparticles were purified and collected using ultracentrifugation (15,000 rpm, 15 min)[5].

Measurement of FRET efficiency of nanosensor.

FRET efficiency of lanthanide-cyanine nanostructures with various MY-1057 concentration were calculated based on the fluorescence lifetime of the DSNP donor by the following equation:

$$\eta = \left(1 - \frac{\tau_{D-A}}{\tau_D}\right) \times 100\%$$

Where h indicates the FRET efficiency, $t_{D\text{-}A}$ and t_D indicates the fluorescence lifetime of DSNP donor at 1060 nm with or without the MY-1057 acceptor, respectively.

Measurement of partition coefficient of MY-dyes.

Each dye was first dissolved in 10 mL n-octyl alcohol at a concentration of 0.2 mg mL^{-1} and then partitioned with 10 mL water. The mass of the dye in water phase were measured after lyophilization. The mass in n-octyl alcohol and water were indicated as M_o and M_w. Partition coefficient (Log *P*) were calculated by the following equation:

$$\text{Log } P = \log\left(\frac{M_o}{M_w}\right)$$

Evaluation of RNS/ROS response of DSNP@MY-1057-GPC-3

Preparation of ROS/RNS solution.

Superoxide ($O_2^{\bullet-}$) was generated from KO_2 dissolved in DMSO.

Hydroxyl radical (•OH) was generated by Fenton reaction. Briefly, ferrous chloride ($FeCl_2$) was added

in the presence of 10 equiv. of H_2O_2. The concentration of •OH was equal to the Fe (II) concentration. The $ONOO^-$ solution was synthesized according to the literature[6]. Briefly, HCl (0.6 M) was added to a mixed solution of H_2O_2 (0.7 M) and $NaNO_2$ (0.6 M), then a NaOH (1.5 M) solution was added. Excess H_2O_2 was removed by eluting the solution through a short column of manganese dioxide. The resulting solution was split into small aliquots and stored at -20 ^oC. By measuring the absorption peak at 302 nm, the concentration of $ONOO^-$ was determined with an standard extinction coefficient of $ONOO^-$ in 0.1 M NaOH solution of 1670 M^{-1} cm^{-1} at 302 nm.

$$C_{ONOO^-} = Abs_{302\ nm}/\ 1.67\ (mM)$$

Evaluation of RNS/ROS response of DSNP@MY-1057-GPC-3.

The response of nanoprobes to $ONOO^-$ and other reactive spices was performed by adding different reactive spices to nanoprobes (8 mg ml^{-1}). Then luminescence lifetime was measured before and after reactive spices addition.

Calculation of $ONOO^-$ concentration

Amount of DSNP@MY-1057-GPC-3 (m/mg) in vitro and in vivo could be measured by ICP-OES. Luminescence lifetime value (τ/μs) could be obtained by time-resolved NIR-II imaging system. Thus the amount of $ONOO^-$ (n/μmol) could be calculated as follows:

1. When amount of nanosensor is 8 mg ml^{-1} (volume of nanosensor=V/L), $ONOO^-$ concentration fits Function 1, which was extracted from Figure 3f.

$$\tau_{ONOO^-}=3\ C_{ONOO^-}+206 \qquad \text{Func. 1}$$

That is

$$C_{ONOO^-}= (\tau_{ONOO^-} -206)/3$$

$$N_{ONOO^-}= C_{ONOO^-}\times V= C_{ONOO^-}= (\tau_{ONOO^-} -206)\times V/3 \text{ (amount of nanosensor: 8V/g)}$$

2. When we obtain a sample with lifetime of τ, nanosensor amount of m, then amount of $ONOO^-$ n could be calculated as:

$$n= [(\tau-206) \times V /3] \times m/(8\times10^3\times V)$$

That is

$$n= (\tau-206)\times m/24000 \qquad \text{Eq. S1}$$

Time-resolved NIR-II imaging system.

Time-resolved NIR-II imaging system has been reported previously[5]. A customized time-gating module was built and coupled to a cooled InGaAs camera (NIRvana: 640, Princeton Instruments; 640 × 512 pixels). The module consists of a camera lens (SWIR-16, Navitar), a focusing lens (f = 20 mm), a high-speed optical chopper (C995, Terahertz Technologies) and a magnifier lens pair (× 10 magnification; f_1 =20 mm and f_2 = 200mm). The object was placed around 100 mm in front of the camera lens. Excitation was provide by an 808 nm diode laser. Emission light collected by the camera lens was passed through a 1 mm pinhole attached in close proximity to the chopper blade, and magnified 10 times to project onto the sensor of the camera. 1000 nm long-pass filter was used for imaging. Synchronization was performed by sending the transistor–transistor logic (TTL) signal output from the chopper to a multifunction I/O device (USB-6353, National Instruments), which generated a delayed TTL signal to trigger the excitation laser. A series of time delays were used to acquire signal corresponding to different sections of the luminescence decay curves, allowing lifetime values to be computed for each pixel.

Region of interest (ROI) for data extraction were marked in the corresponding figures. In Figure 3, ROI for lifetime data extraction were marked with white dashed box in Figure 3a. In Figure 4, tumor ROI and normal hepatic tissue ROI for lifetime data extraction were marked with red dashed circle and violet dashed circle, respectively, in Figure 4b and 4f. Lifetime values were taken from pixels in ROI of the lifetime images and indicated as mean ± s.d.. It should be noticed that “counts” on the vertical scale is used to represent the normalized pixel number to evaluate the lifetime distribution evaluation.

Tissue phantom imaging study

1% Intralipid® was chosen as a simulated tissue due to its similar scattering characteristics. Capillary tube filled with RNS responded DSNP@MY-1057-GPC-3 were encapsulated for imaging. The capillary tube was then placed under a cylindrical culture dish and covered with different depth of 1% Intralipid®. 1000 nm long-pass filter was used for imaging. To obtain the penetration depth information, the average intensity was obtained from the same ROI of various depths. Exposure time was 5,000 ms. All images were background and blemish corrected within the LightField imaging software and processed with Matlab.

Cytotoxicity assay

Human umbilical vein endothelial cells (HUVEC) and human hepatocellular carcinoma HepG-2 cells were provided by Stem Cell Bank, Chinese Academy of Science. Cells were excluded mycoplasma contamination by mycoplasma Detection Kit. Both of the cells were cultured in Dulbecco's Modified Eagle medium (DMEM) supplemented with 10% FBS and 1% Penicillin-Streptomycin at 37 °C in a humidified atmosphere of 5% CO_2. HUVEC and HepG-2 cells were cultured in a 96-well plate (8×10^3 cells/well) after 24 h incubation, the medium was replaced with 100 μL of fresh DMEM containing DSNP@MY-1057-GPC-3 with concentrations of 10, 20, 50, 100, 200, 500, 1000 and 2000 μg ml^{-1}, respectively. Cells were incubated further for 24 h. To detect the cytotoxicity, 10 μL of Cell Counting Kit-8 (CCK-8) solution was added to each well of the microliter plate and the plate was incubated in the CO_2 incubator for additional 4 h. Enzyme dehydrogenase in living cells was oxidized by this kit to orange carapace. The quality was assessed calorimetrically by using a multi-reader (TECAN, Infinite M200, Germany). The measurements were based on the absorbance values at 450 nm. Following formula was used to calculate the viability of cell growth:

Viability (%) = (mean absorbance value of treatment group/mean absorbance value of control group) × 100%.

Animal model

All animal experiments were in agreement with the guidelines of Fudan University's Administrative panel on Laboratory Animal Care. Five weeks old female nude mice were purchased from Shanghai SLAC Laboratory animal CO. Ltd. And the animal experiments were permitted by the Shanghai Science and Technology Committee. To build in situ HCC model, mice were anesthetized with isoflurane, placed in a supine position and limbs were fixed on a heated surgical pad using low-tack adhesive tape. The abdomen of mice was scrubbed with iodine scrub and alcohol prior to the surgery. A midline incision was made and liver was exposed, then a series amount of human hepatocellular carcinoma HepG-2 cells were injected into liver tissue of nude mice to mimic naturally occurring

tumors with different sizes.

Note S1. After intravenously administration of DSNP@MY-1057-GPC-3 nanosensors, the liver as a representative organ of reticuloendothelial system (RES) would highly capture the luminescence nanosensors with hydrodynamic diameter of ~50 nm. As a result, tumor lesions could be hardly distinguished by the luminescence intensity signals due to the high background signals from the nanosensors captured by healthy hepatic tissue. On the contrary, tumor lesions could be distinguished from healthy hepatic tissue due to the recovery lifetime values during luminescence lifetime-based imaging. Thereby, HCC model is the most appropriate model to exhibit the advantage of sensitivity and reliability of luminescence lifetime-based imaging.

In vivo imaging

All NIR-II images were collected on a home-built small animal imaging system with 640×512 pixel 2D InGaAs NIRvana camera, exposure time was 300 ms. All NIR-II lifetime images were acquired on the above-mentioned time-resolved NIR-II imaging system, exposure time was 20,000 ms. Images were processed with the LightField imaging software, ImageJ and MATLAB.

Characterization

Transmission electron microscopy (TEM) test were performed using a JEM-2100F transmission electron microscope with an accelerating voltage of 200 kV equipped with a post column Gatan imaging filter (GIF-Tri-dium). Absorption spectra were collected by using a PerkinElmer Lambda 750S UV-visible-NIR spectrometer with a 300 nm/min scan rate. The emission spectra were obtained on an Edinburgh Instruments FLS980 fluorescence spectrometer (unless otherwise specified, all spectra were collected under identical experimental conditions). The distribution of nanoprobes were determined

by measuring Y^{3+} content in different organs by ICP-OES using iCAP 7400, Thermo Fisher Scientific. Isothermal titration calorimetry (ITC) experiments were conducted on a MicroCal VP-ITC system at 20.00 ± 0.01°C. MRI results were acquired by CG NOVILA 7.0T (T_2–weighted images) from Shanghai Chenguang Medical Technologies Co.,Ltd.

Part B: Figure Ss

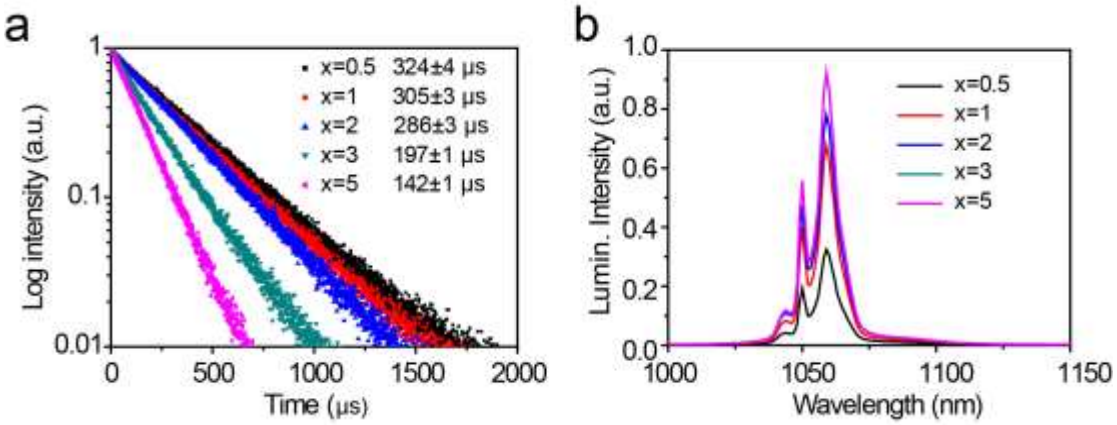

Figure S1. Luminescence decay curves (a) and luminescence intensity (b) of $NaYF_4$@$NaYF_4$:x%Nd nanoparticles (abbreviated as Y@Y:x%Nd), x=0.5, 1, 2, 3 and 5. Lifetimes are indicated as mean ± s.d. (n=3).

Luminescence lifetime were close when x=0.5 and x=1, but luminescence intensity of Y@Y:0.5%Nd nanoparticles decreased obviously compared to that of Y@Y:1%Nd. Thus $NaYF_4$@$NaYF_4$:1%Nd was finally chosen as energy donor in the fluorescence resonance energy transfer (FRET) system.

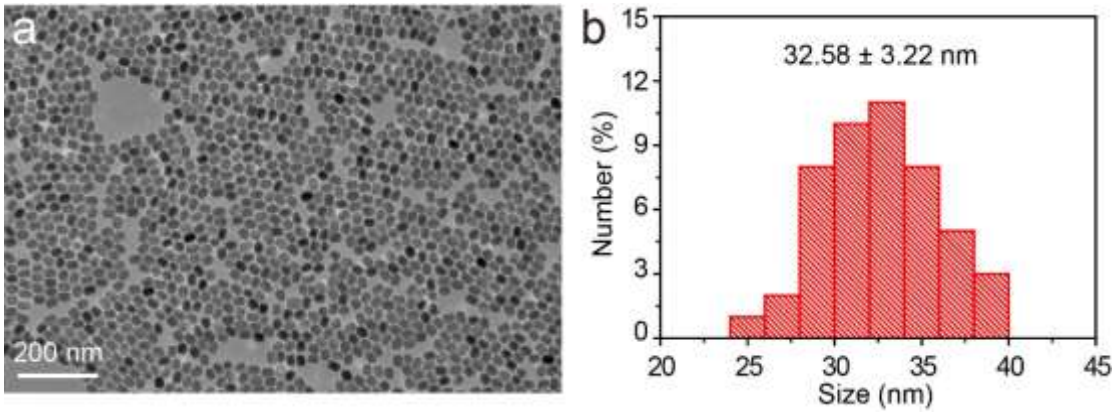

Figure S2. Transmission electron microscopy (TEM) image (a) and size distribution results (b) of as made DSNPs.

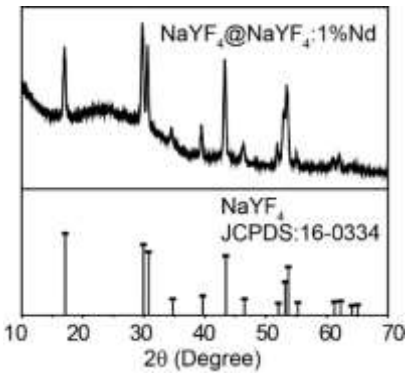

Figure S3. XRD patterns of β- $NaYF_4$@$NaYF_4$:1%Nd.

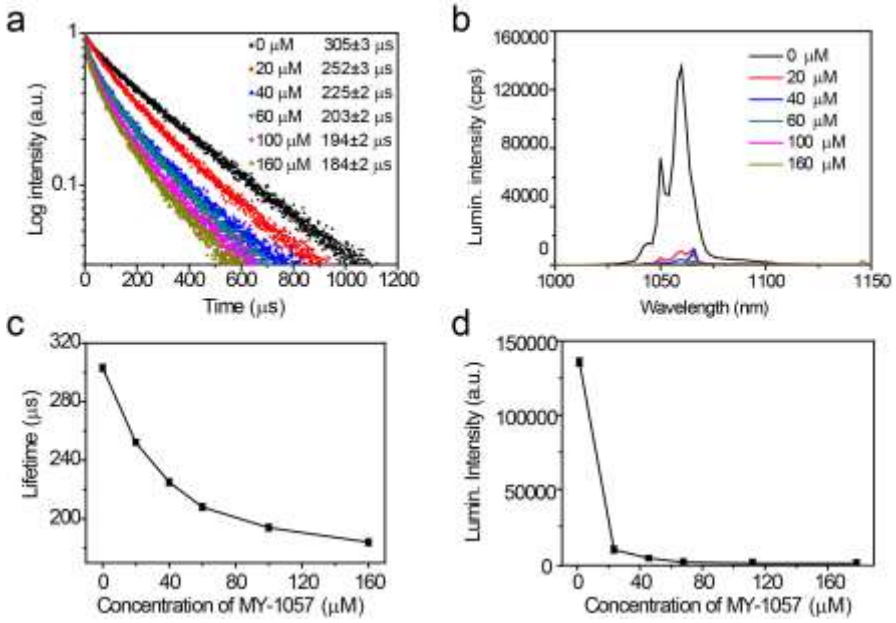

Figure S4. Optimizing the MY-1057 amount encapsulated into DSNPs. a) Luminescence decay curves of DSNPs encapsulated with various amount of MY-1057. b) Luminescence spectra of DSNPs encapsulated with various amount of MY-1057. c) Luminescence lifetime of DSNPs encapsulated with various MY-1057 amount as a function of MY-1057 concentration. d) Luminescence intensity of DSNPs encapsulated with various MY-1057 amount as a function of MY-1057 concentration. Error bars: mean ± s.d. (n=3). Concentration of DSNPs: 8 mg ml^{-1}.

Luminescence lifetime of DSNPs decreased obviously with the increased amount of MY-1057. However, when concentration of MY-1057 reached 60 μM, the rate of decrease has slowed down. To ensure the sensitivity of $ONOO^-$ response, 60 μM MY-1057 was chosen to encapsulate into DSNPs.

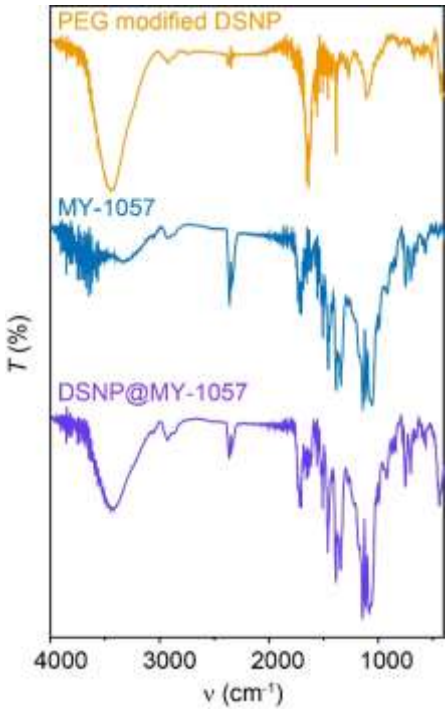

Figure S5. Fourier transform infrared (FTIR) spectrum of synthesized PEG modified DSNP, MY-1057 dye, and DSNP@MY-1057.

The main vibration modes of PEG modified DSNP contained ν(N-H) at 3448 cm^{-1}, ν(C-H) at 2932 cm^{-1}, 1380 cm^{-1}, 1096 cm^{-1}, and ν(C=O) at 1654 cm^{-1}. The main vibration modes of MY-1057 contained ν(O-H) at 3332 cm^{-1}, 2896 cm^{-1}, ν(C=C) at 2360-2330 cm^{-1}, ν(C=O) at 1709 cm^{-1}, ν(C-N) at 1383-1340 cm^{-1}, and ν(C-C) and ν(C-N) at 1136-1057 cm^{-1}. The main vibration modes of DSNP@MY-1057 contains all the vibration modes observed in PEG modified DSNP and MY-1057 dye, illustrating the MY-1057 dye was successfully encapsulated on the surface of DSNP.

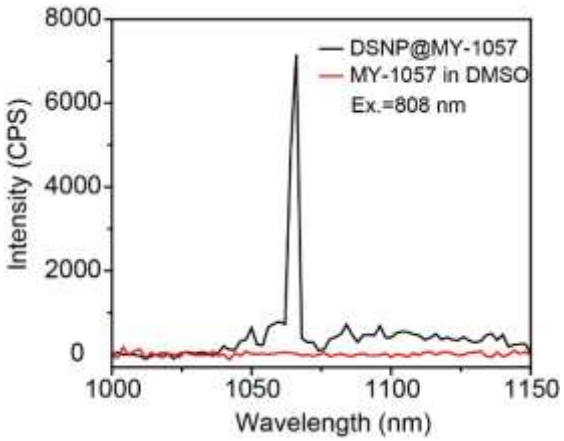

Figure S6. Emission spectra of DSNP@MY-1057 in water and MY-1057 dye in DMSO. Ex. 808 nm, concentration of MY-1057: 60 μM.

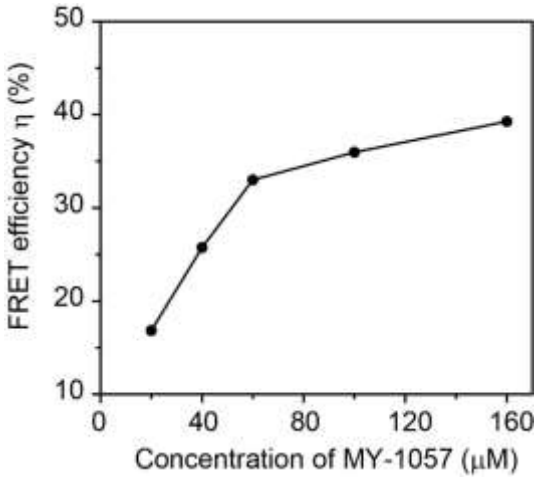

Figure S7. FRET efficiency of DSNP@MY-1057 nanostructures with various MY-1057 concentration.

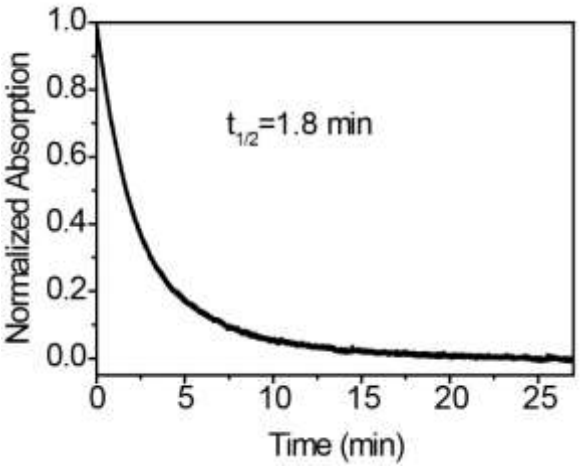

Figure S8. Reaction kinetics of MY-1057 and $ONOO^-$.

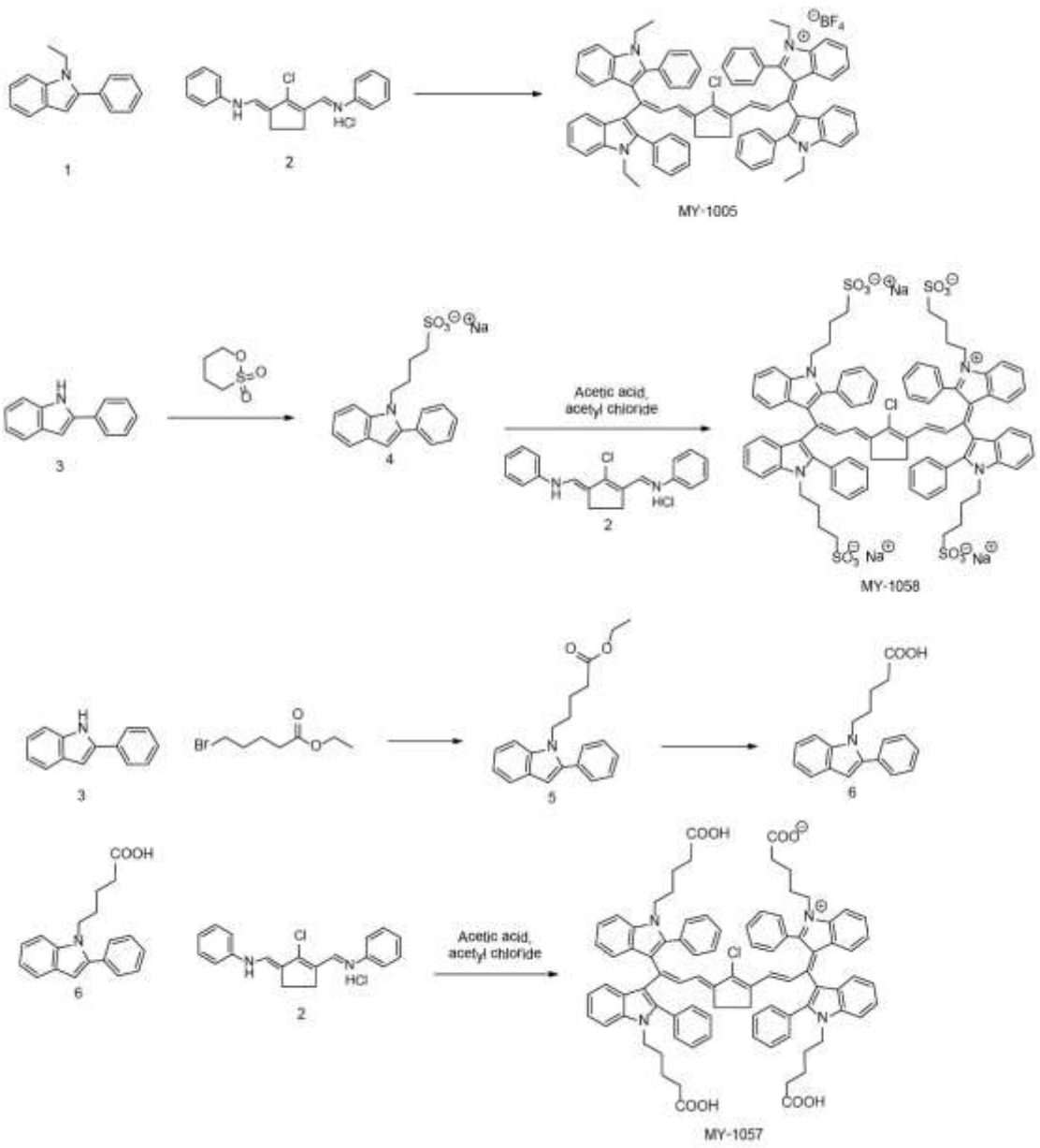

Figure S9. Synthesis route of MY-dyes.

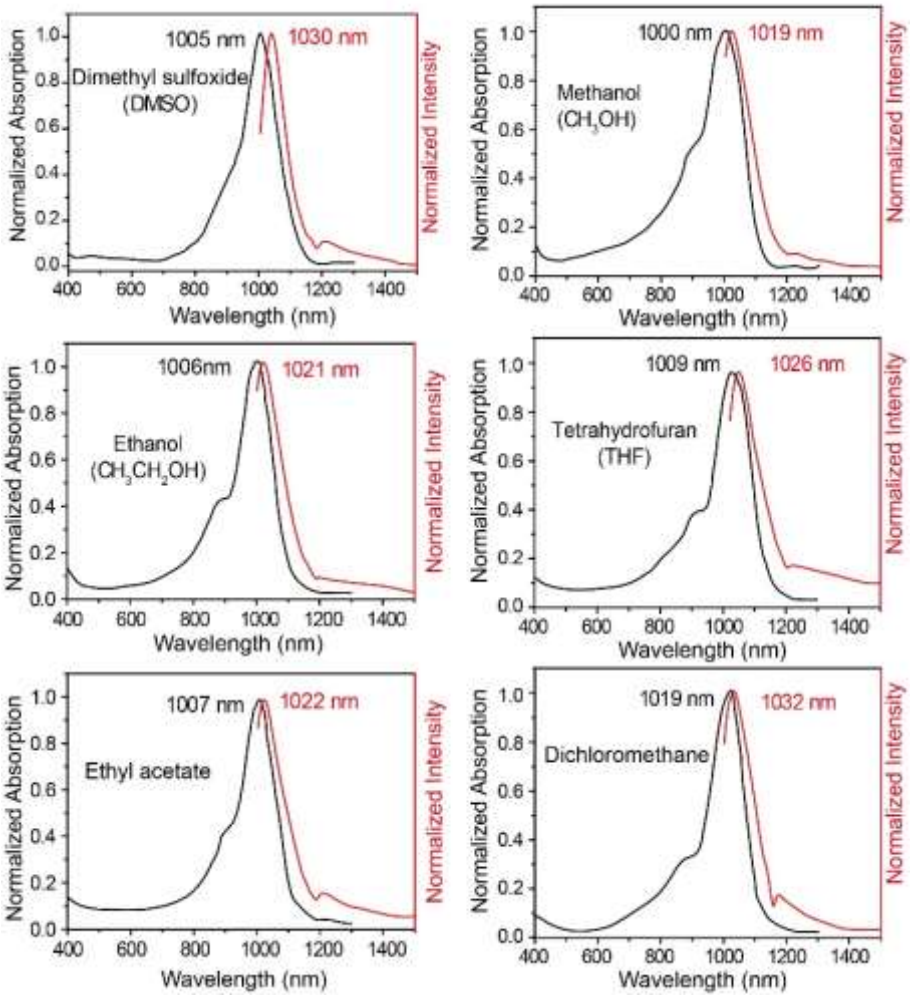

Figure S10. Absorption and fluorescence emission spectra of MY-1005 in different solvents as indicated. The fluorescence emission spectra were obtained under 980 nm laser excitation.

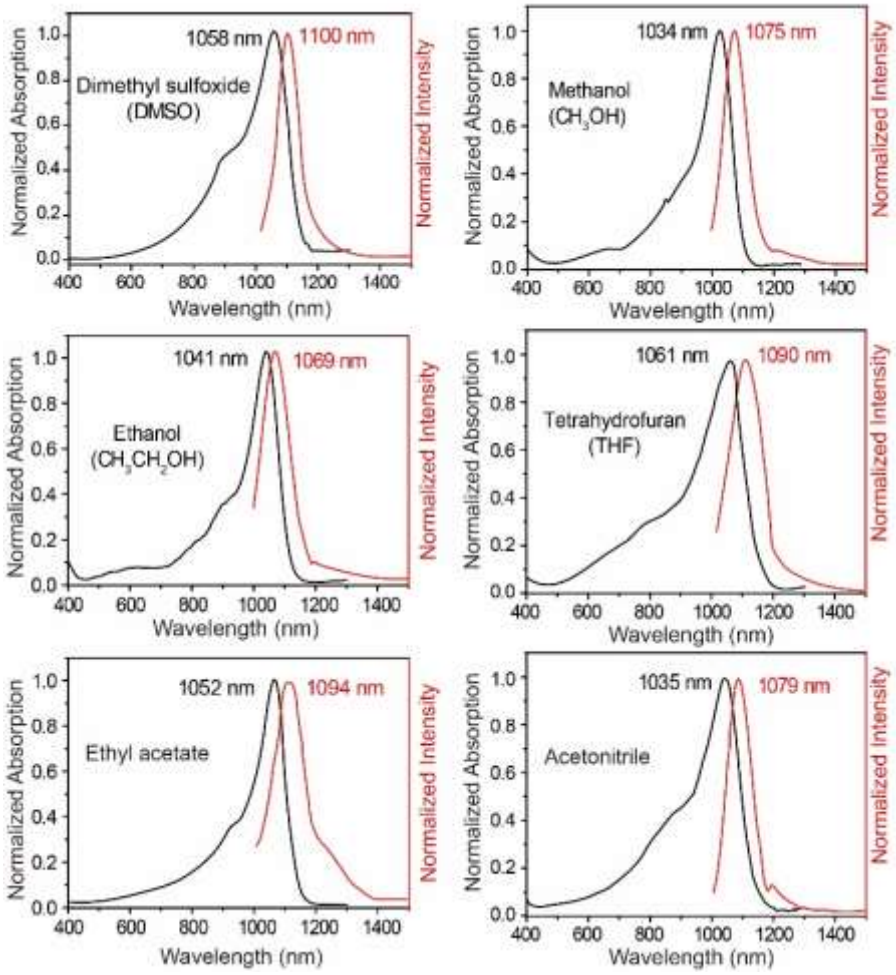

Figure S11. Absorption and fluorescence emission spectra of MY-1058 in different solvents as indicated. The fluorescence emission spectra were obtained under 980 nm laser excitation.

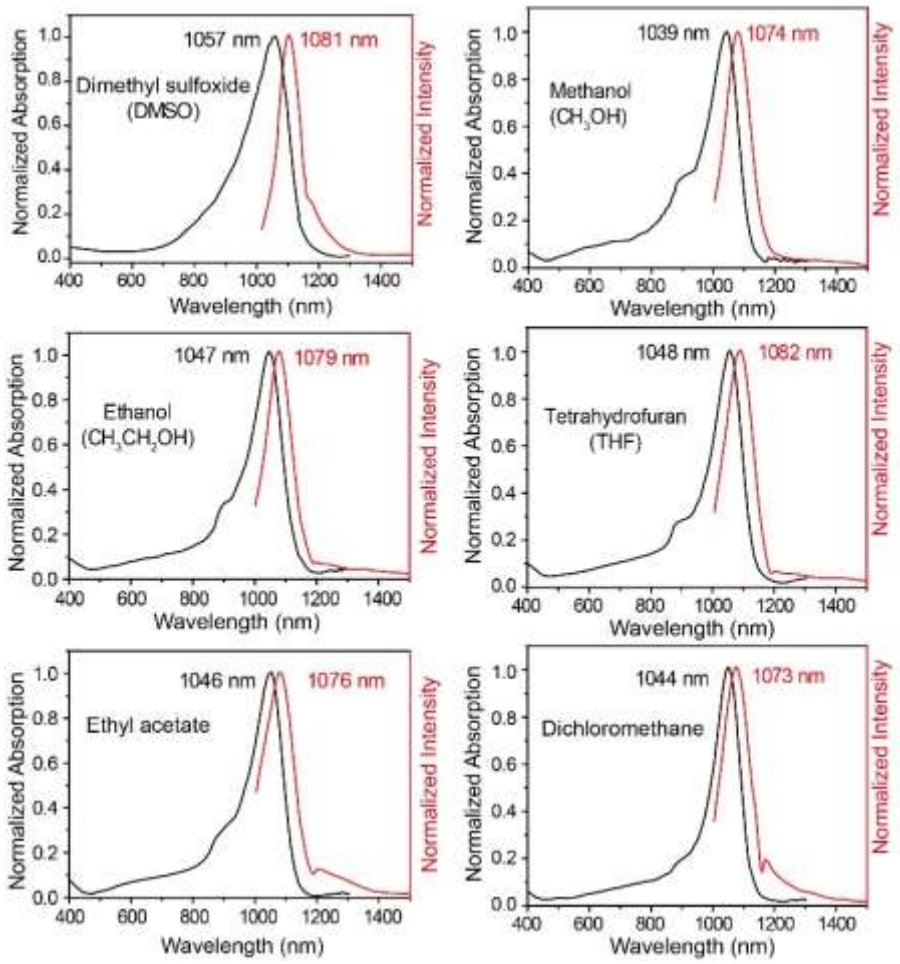

Figure S12. Absorption and fluorescence emission spectra of MY-1057 in different solvents as indicated. The fluorescence emission spectra were obtained under 980 nm laser excitation.

Table S1. Photophysical characterization of MY-1005

Solvent	λ_{abs} (nm) [a]	ε_{max}($\times 10^5$ M^{-1} cm^{-1})	λ_{em} (nm) [b]	Φ_f (%)[c]
Dimethyl sulfoxide	1005	1.42	1030	0.90±0.02
Methanol	1000	1.61	1019	0.21±0.01
Ethanol	1006	1.51	1021	0.37±0.01
Tetrahydrofuran	1009	1.54	1026	0.28±0.01
Ethyl acetate	1007	1.53	1022	0.41±0.02
Dichloromethane	1019	1.55	1032	0.52±0.02

[a] The maximal absorption of the dye. [b] The maximal emission of the dye. [c] The relative fluorescence quantum yield (0.05%) by using IR-26 in 1,2-dichloroethane as a reference system.

Table S2. Photophysical characterization of MY-1058

Solvent	λ_{abs} (nm) [a]	ε_{max}($\times 10^5$ M^{-1} cm^{-1})	λ_{em} (nm) [b]	Φ_f (%)[c]
Dimethyl sulfoxide	1058	1.48	1100	3.89±0.11
Methanol	1034	1.66	1075	1.22±0.08
Ethanol	1041	1.57	1069	2.66±0.09
Tetrahydrofuran	1061	1.24	1090	0.41±0.01
Ethyl acetate	1052	1.11	1094	0.35±0.01
Acetonitrile	1035	1.23	1079	0.96±0.01

[a] The maximal absorption of the dye. [b] The maximal emission of the dye. [c] The relative fluorescence quantum yield (0.05%) by using IR-26 in 1,2-dichloroethane as a reference system.

Table S3. Photophysical characterization of MY-1057

Solvent	λ_{abs} (nm) [a]	ε_{max}($\times 10^5$ M^{-1} cm^{-1})	λ_{em} (nm) [b]	Φ_f (%)[c]
Dimethyl sulfoxide	1057	1.07	1081	0.71±0.01
Methanol	1039	1.87	1074	0.35±0.00
Ethanol	1047	1.75	1079	0.46±0.01
Tetrahydrofuran	1048	1.95	1082	0.37±0.02
Ethyl acetate	1046	1.67	1076	0.49±0.03
Dichloromethane	1044	1.86	1073	0.38±0.02

[a] The maximal absorption of the dye. [b] The maximal emission of the dye. [c] The relative fluorescence quantum yield (0.05%) by using IR-26 in 1,2-dichloroethane as a reference system.

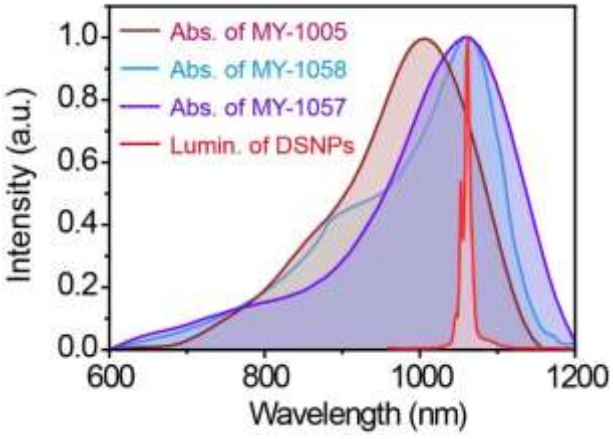

Figure S13. Overlap of the MY-dyes absorption spectra and DSNPs luminescence emission spectrum.

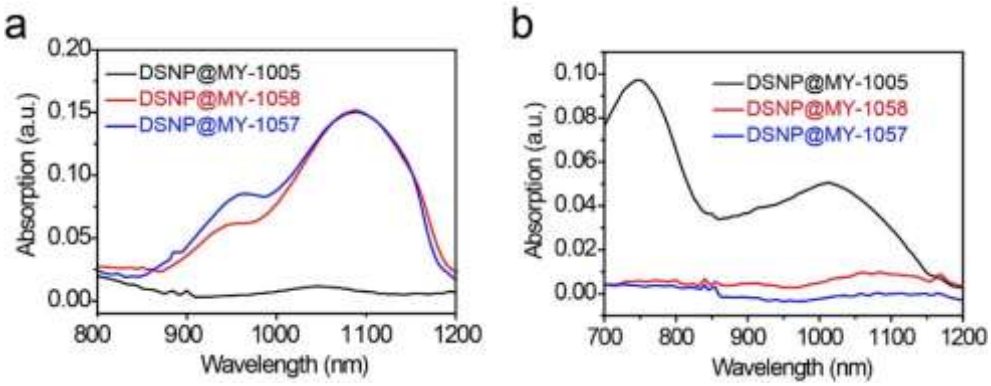

Figure S14. Absorption spectra of nanoparticles (a) and supernate (b) during fabrication of DSNP@MY-1005, DSNP@MY-1058 and DSNP@MY-1057.

MY-1005 was hardly detected on DSNPs while amount of MY-1005 could be detected in the supernate, indicating that few MY-1005 was encapsulated into DSNPs. And MY-1058 and MY-1057 were on the opposite, indicating that most MY-1058 and MY-1057 were encapsulated into DSNPs. Concentration of MY-1005, MY-1058 and MY-1057: 60 μM, concentration of DSNPs: 3 mg ml^{-1}.

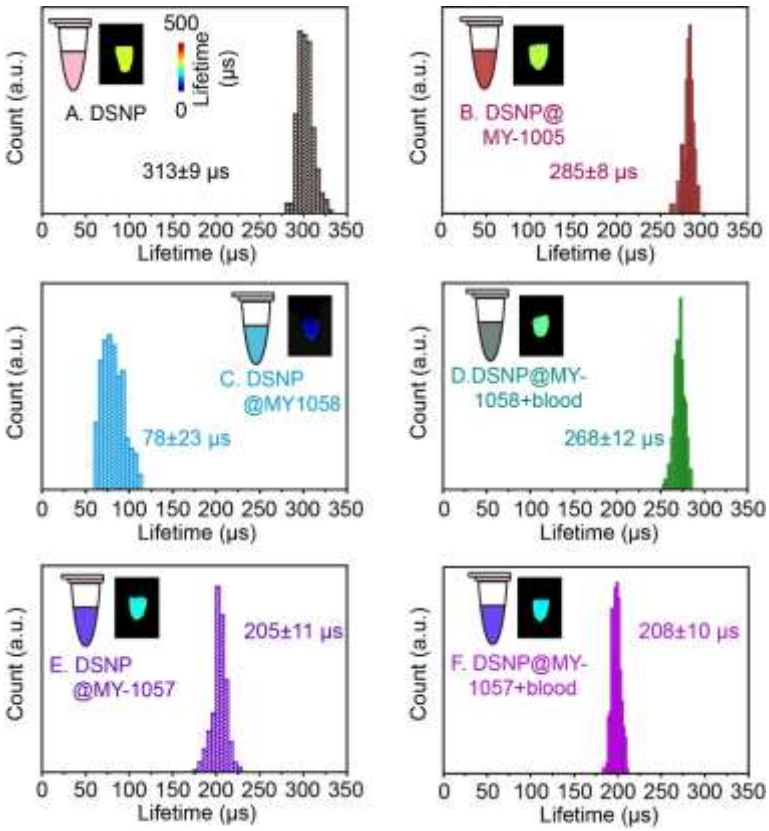

Figure S15. Lifetime distribution extracted from lifetime imaging of sample A-F in Figure 2c. Luminescence lifetime was indicated as mean ± s.d., taken from pixels corresponding to each tube in the lifetime images.

Table S4. Calculation of Log*P* of COOH-PEG_{5000}-OCH_3 and MY-dyes

	mass in n-octyl alcohol (mg)	mass in water (mg)	Log*P*
	1.086	3.914	-0.556
COOH-PEG_{5000}-OCH_3	0.978	4.022	-0.614
	1.152	3.848	-0.523
	1.529	0.471	0.511
MY-1005	1.588	0.412	0.585
	1.471	0.529	0.444
	0.154	1.846	-1.078
MY-1058	0.124	1.876	-1.179
	0.169	1.831	-1.034
	1.111	0.889	0.096
MY-1057	1.089	0.911	0.077
	1.053	0.947	0.046

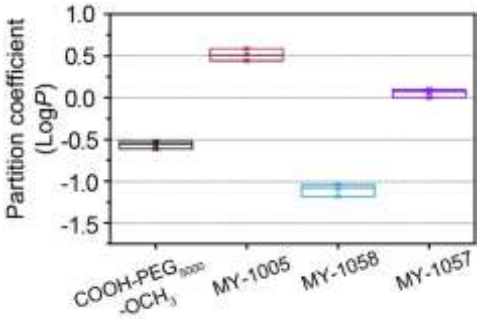

Figure S16. Partition coefficient (Log *P*) of COOH-PEG_{5000}-OCH_3 and MY-dyes. n=3.

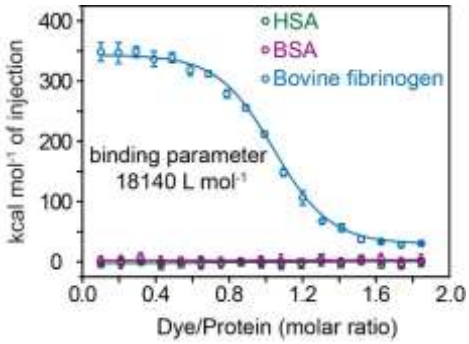

Figure S17. Measurement of binding ability between MY-1058 and protein (HSA, BSA and bovine fibrinogen). Isothermal titration calorimetry (ITC) data titration results of titration of MY-1058 (0.1 mM) into 0.01 mM protein at 20°C in aqueous solution. Error bars: means ± s.d. (n=3).

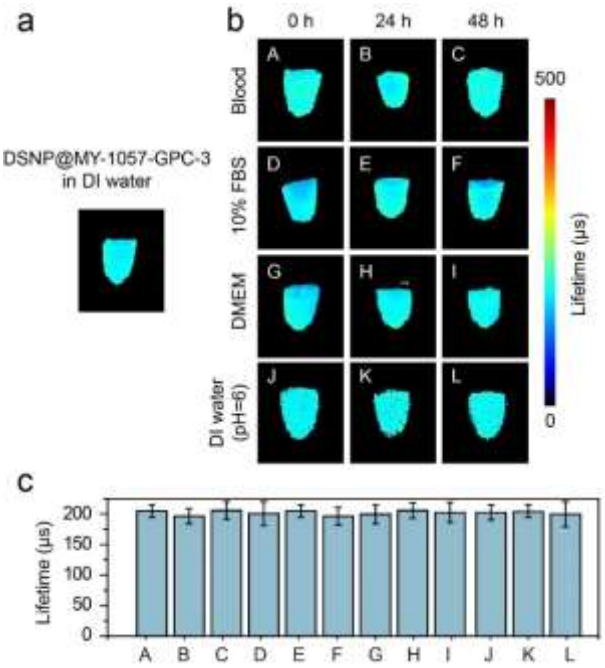

Figure S18. a) Luminescence lifetime of DSNP@MY-1057-GPC-3 in deionized (DI) water. b) Luminescence lifetime of DSNP@MY-1057-GPC-3 in blood, 10% fetal bovine serum (FBS) and cell culture (DMEM) for 48 h. c) Luminescence lifetime value of sample A-I in (b). Luminescence lifetime was indicated as mean ± s.d., taken from pixels corresponding to each tube in the lifetime images.

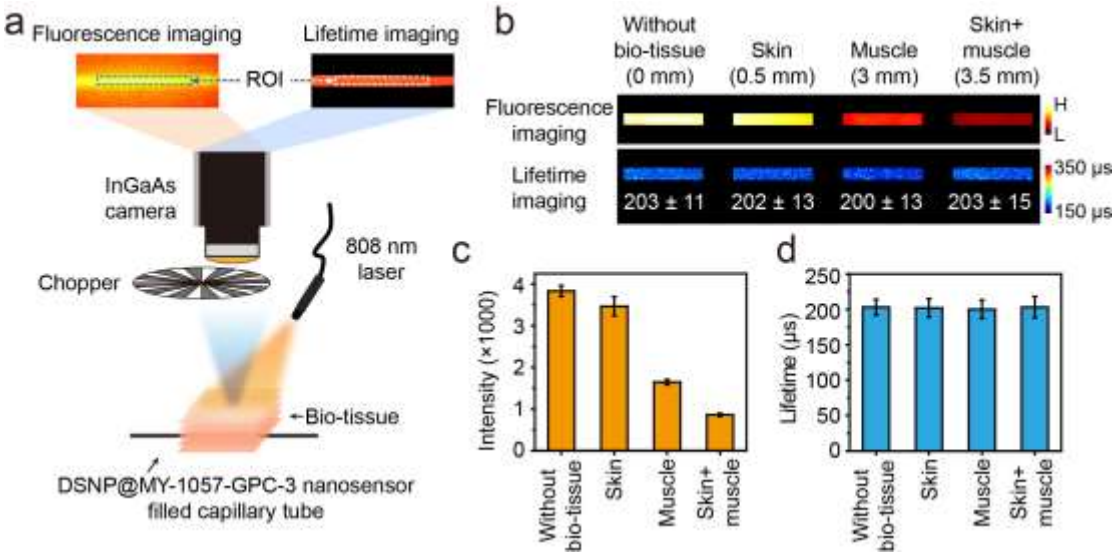

Figure S19. a) Experiment setup for intensity- and lifetime-based imaging of capillary under bio-tissues. ROI for data extraction was marked with blue and white dash box. b) Intensity- and lifetime-based imaging results of DSNP@MY-1057-GPC-3 contained capillaries under bio-tissues. c, d) luminescence intensity and lifetime values of DSNP@MY-1057-GPC-3 nanosensors acquired from (b). Error bars, mean ± s.d..

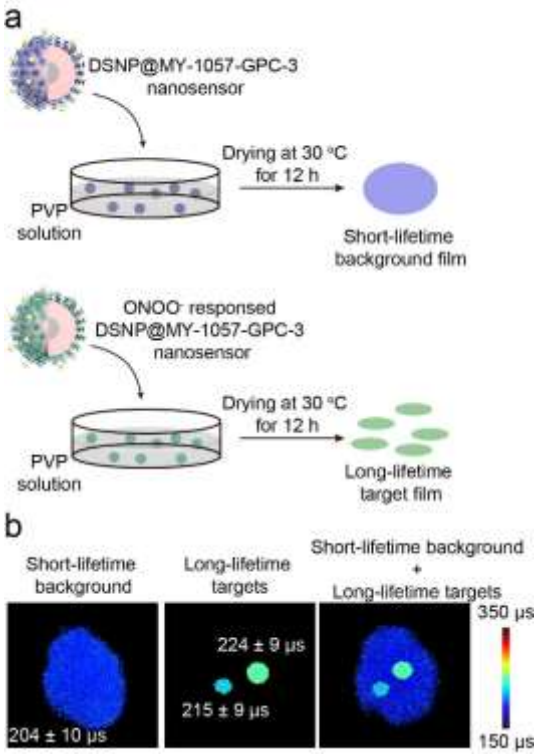

Figure S20. a) Fabrication procedure of the short-lifetime background and long-lifetime target films. b) Lifetime imaging results of short-lifetime background film, long-lifetime target films and overlapped films.

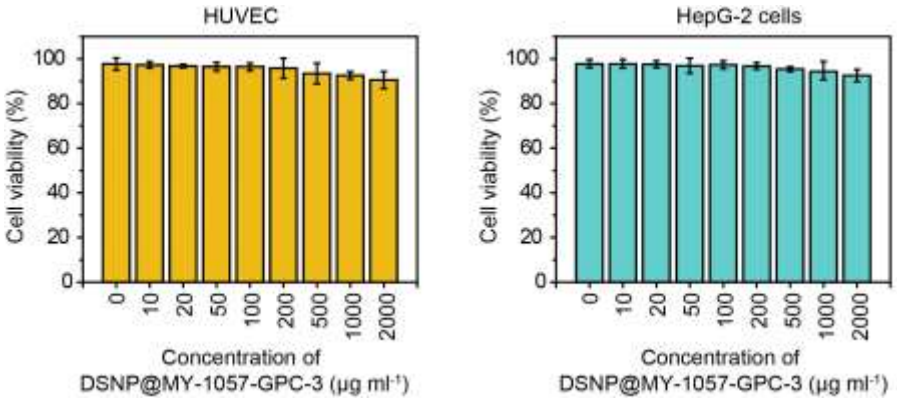

Figure S21. Cell viability of human umbilical vein endothelial cells (HUVEC) and human hepatocellular carcinoma HepG-2 cells after 24 h incubation with DSNP@MY-1057-GPC-3 at different concentrations. Error bars, mean ± s.d. (n = 6).

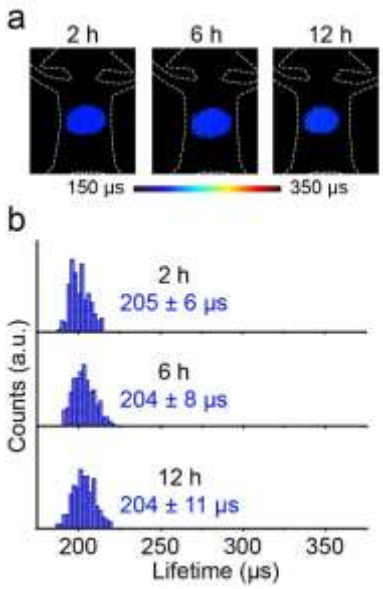

Figure S22. a) Luminescence lifetime imaging of healthy mouse liver at 2 h, 6 h and 12 h after DSNP@MY-1057-GPC-3 administration. b) Lifetime distribution meatured in mouse liver at various time points as indicated.

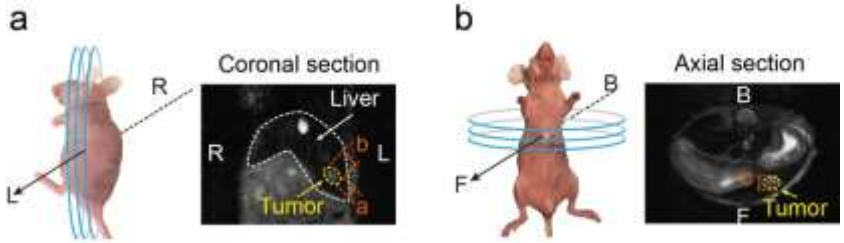

Figure S23. Illustration of tumor size measurement from MRI images.

"a, b" stands for the tumor size in length and width measured from the coronal section, while "c" stands for the tumor thickness measured from the axial section. And the tumor size were calculated by the following equation:

$$V = \frac{1}{6}\pi abc$$

Where V stands for the tumor volume, a, b and c stands for the length, width and thickness measured from the coronal and axial section as indicated.

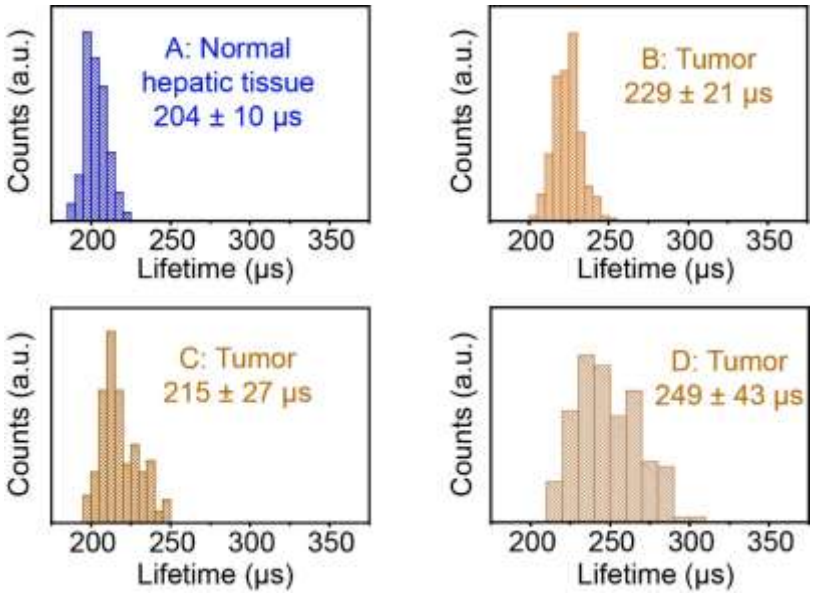

Figure S24. Lifetime distribution of ROI A-D indicated in Figure 4f. Lifetime values were indicated as mean ± s.d..

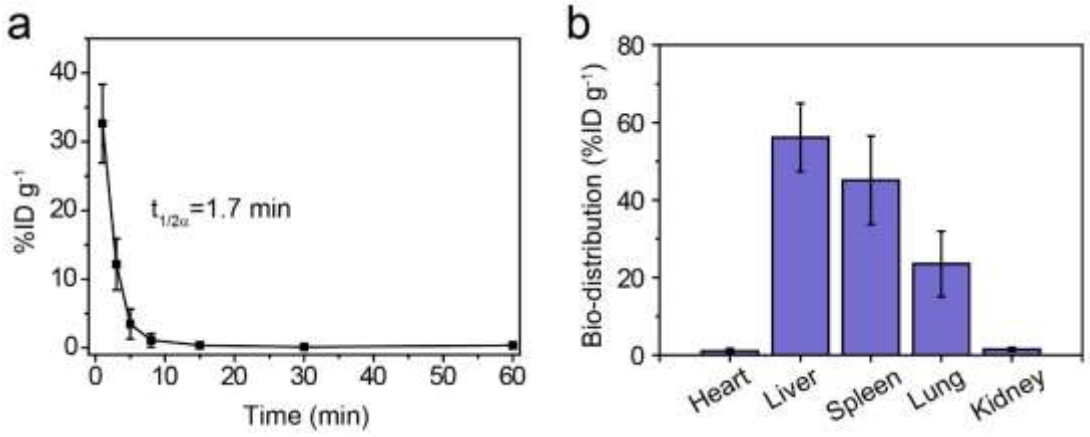

Figure S25. a) Pharmacokinetics of DSNP@MY-1057-GPC-3 in blood after intravenous (i.v.) injection. b) Bio-distribution of DSNP@MY-1057-GPC-3 at 24 h post-injection.

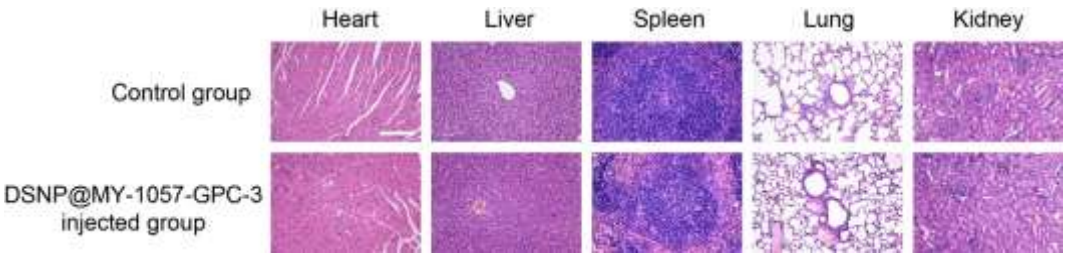

Figure S26. H&E staining results of control mouse organs (above) and mouse organs at 24 h after

DSNP@MY-1057-GPC-3 administration (below). Scale bar: 200 μm.

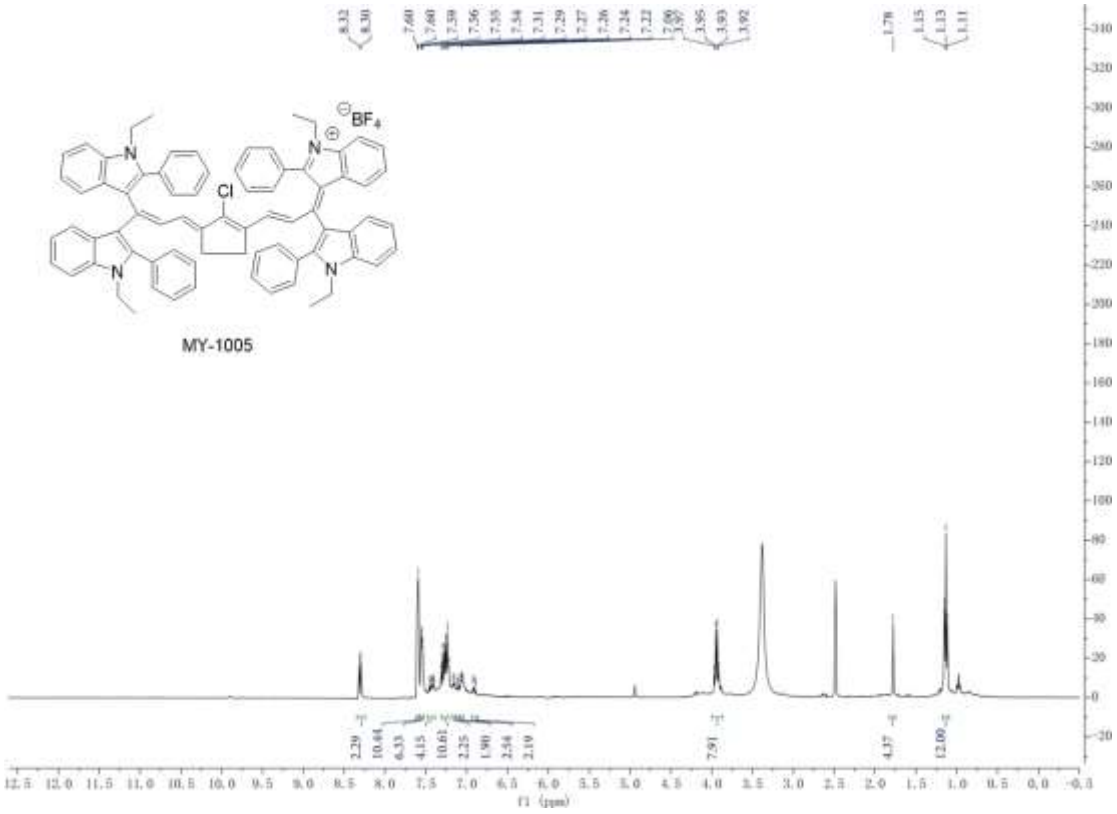

Figure S27. The ^{1}H-NMR spectrum of **MY-1005** in DMSO-d_6.

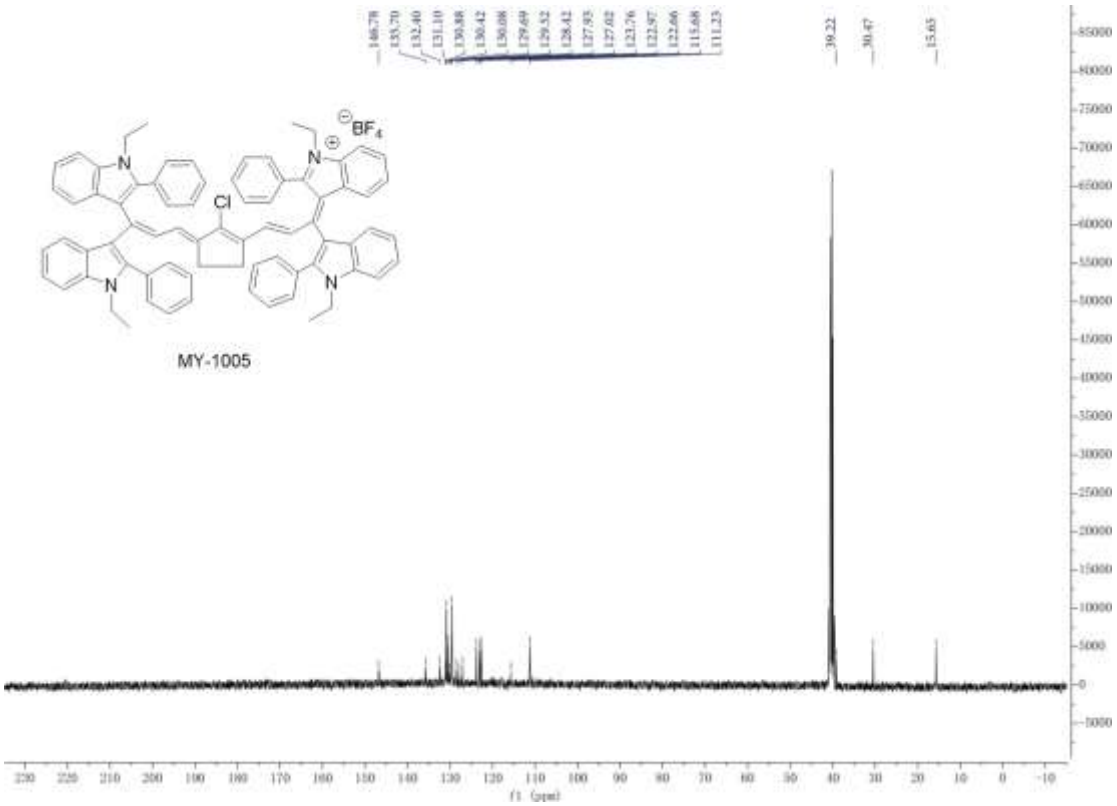

Figure S28. The ^{13}C-NMR spectrum of **MY-1005** in DMSO-d_6.

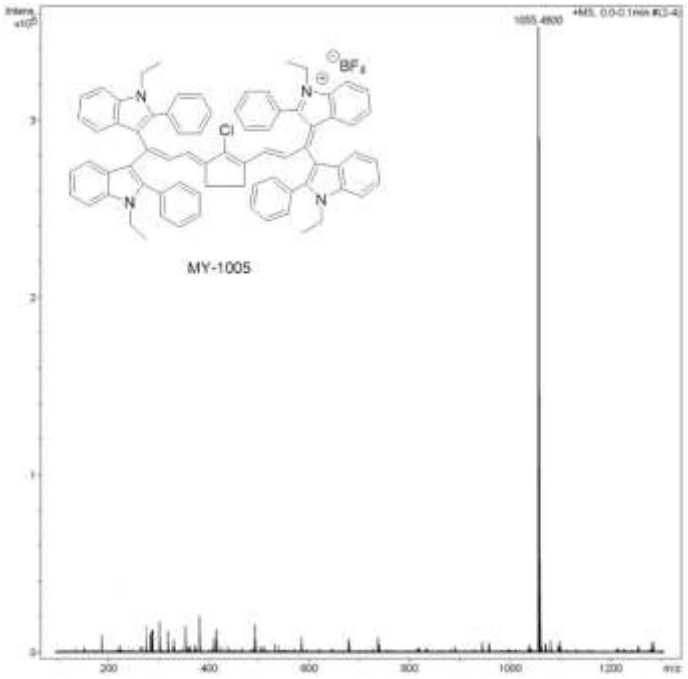

Figure S29. The MS of **MY-1005**.

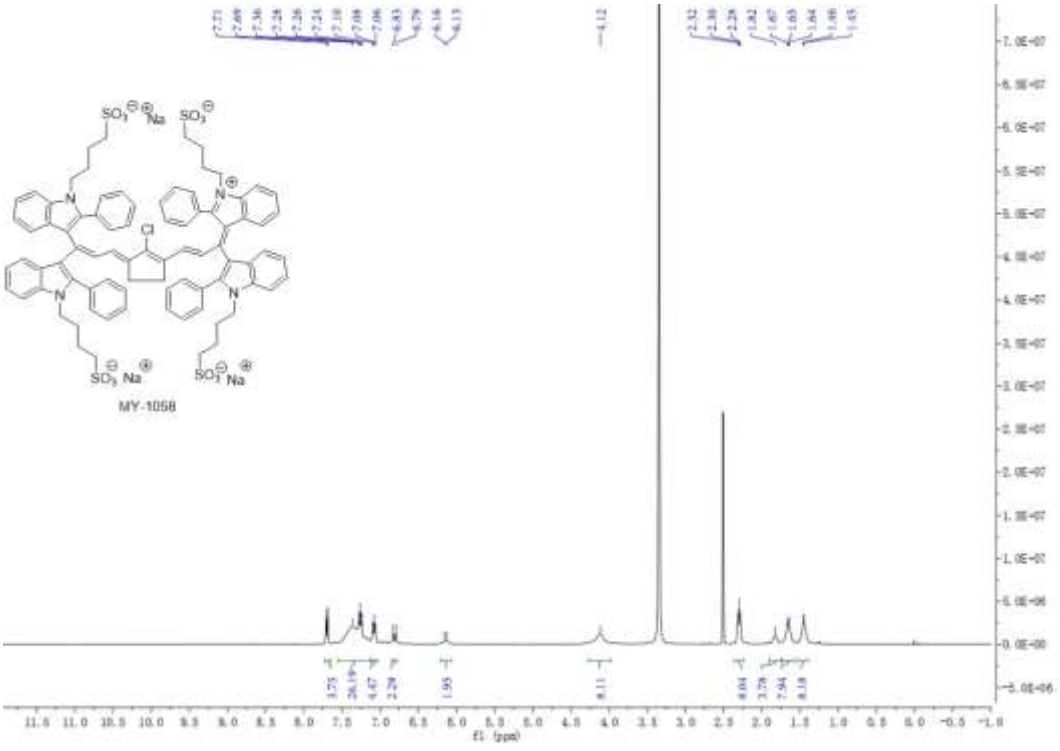

Figure S30. The ^{1}H-NMR spectrum of **MY-1058** in DMSO-d_6.

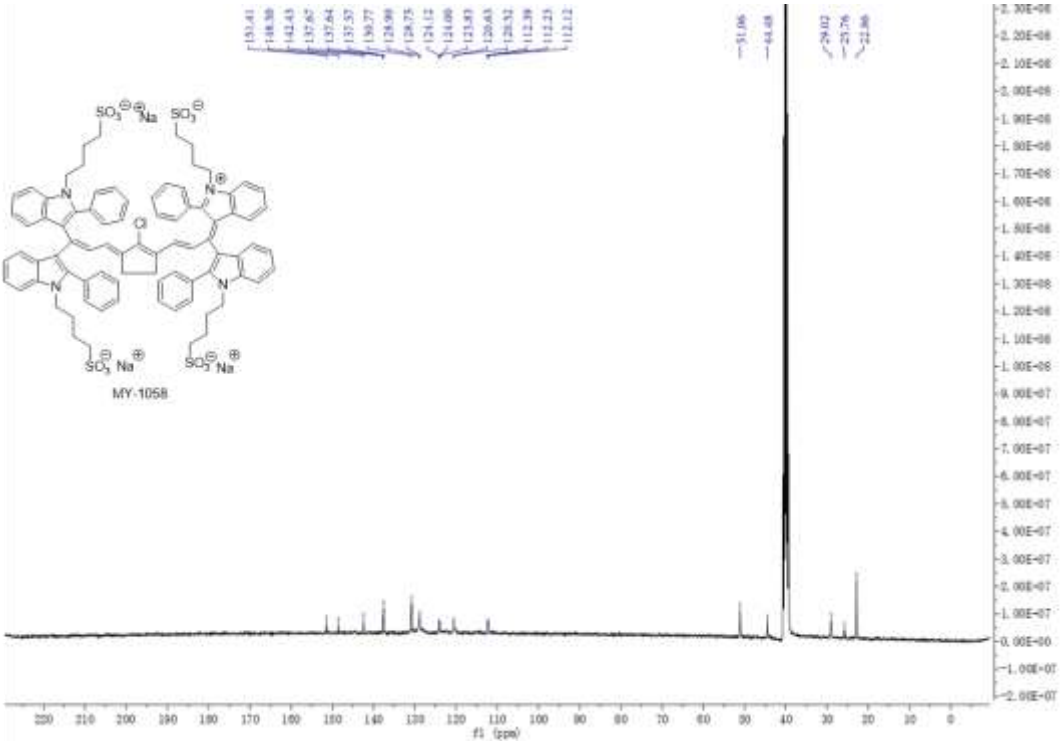

Figure S31. The ^{13}C-NMR spectrum of **MY-1058** in DMSO-d_6.

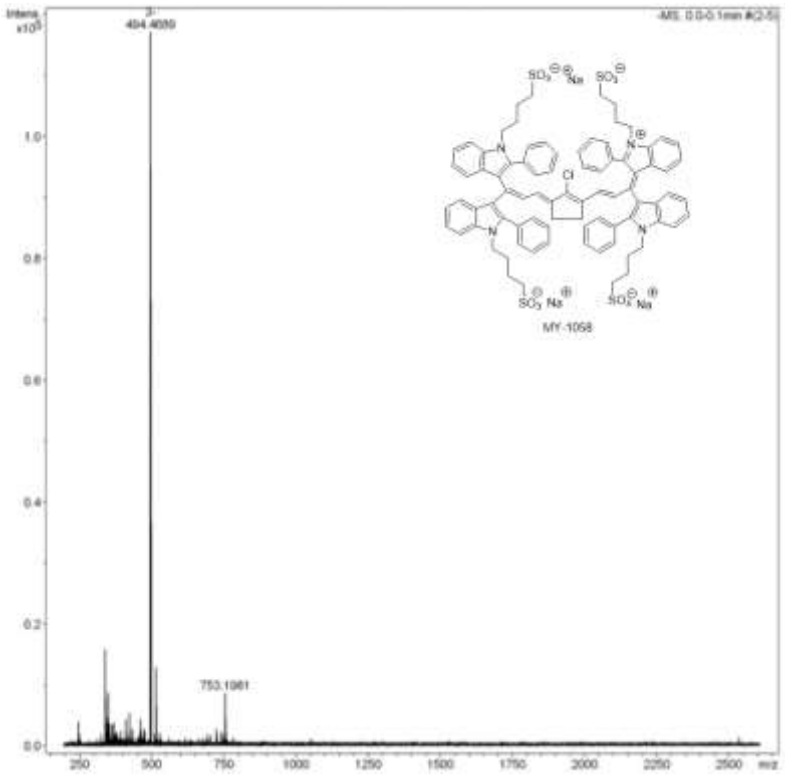

Figure S32. The MS of **MY-1058**.

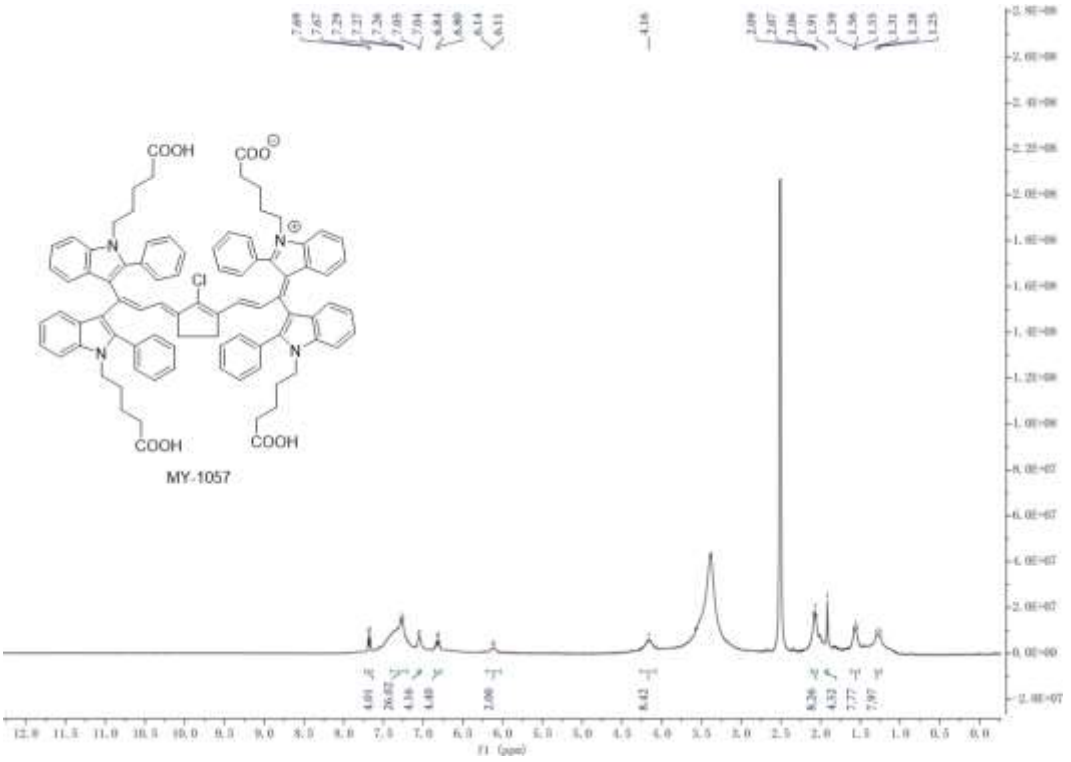

Figure S33. The ^{1}H-NMR spectrum of **MY-1057** in DMSO-d_6.

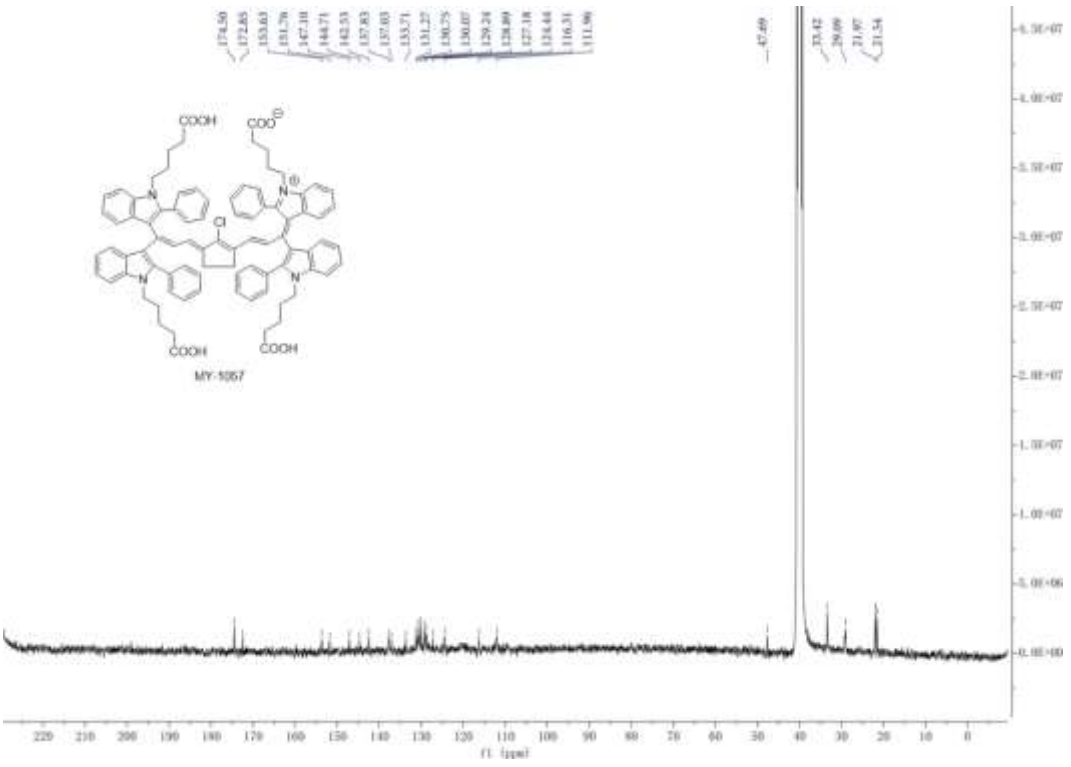

Figure S34. The ^{13}C-NMR spectrum of **MY-1057** in DMSO-d_6.

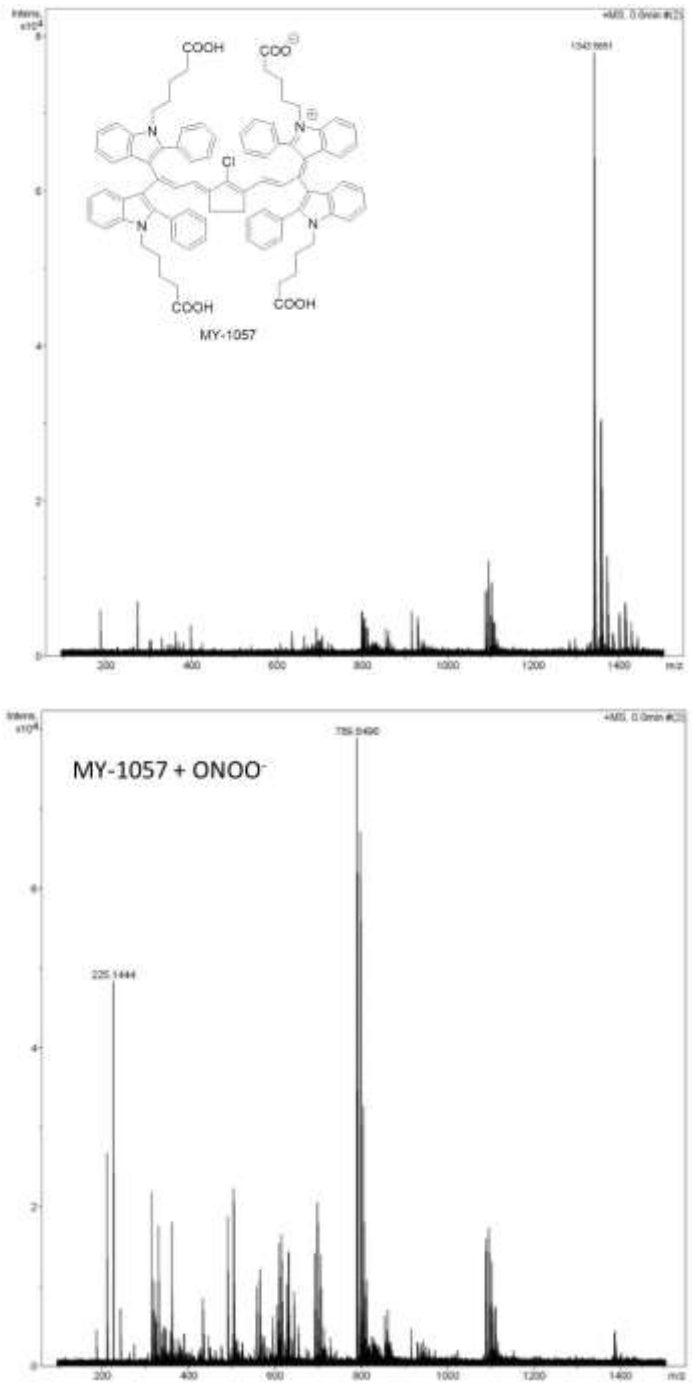

Figure S35. The MS of MY-1057 before (up) and after (down) reacting with $ONOO^-$.

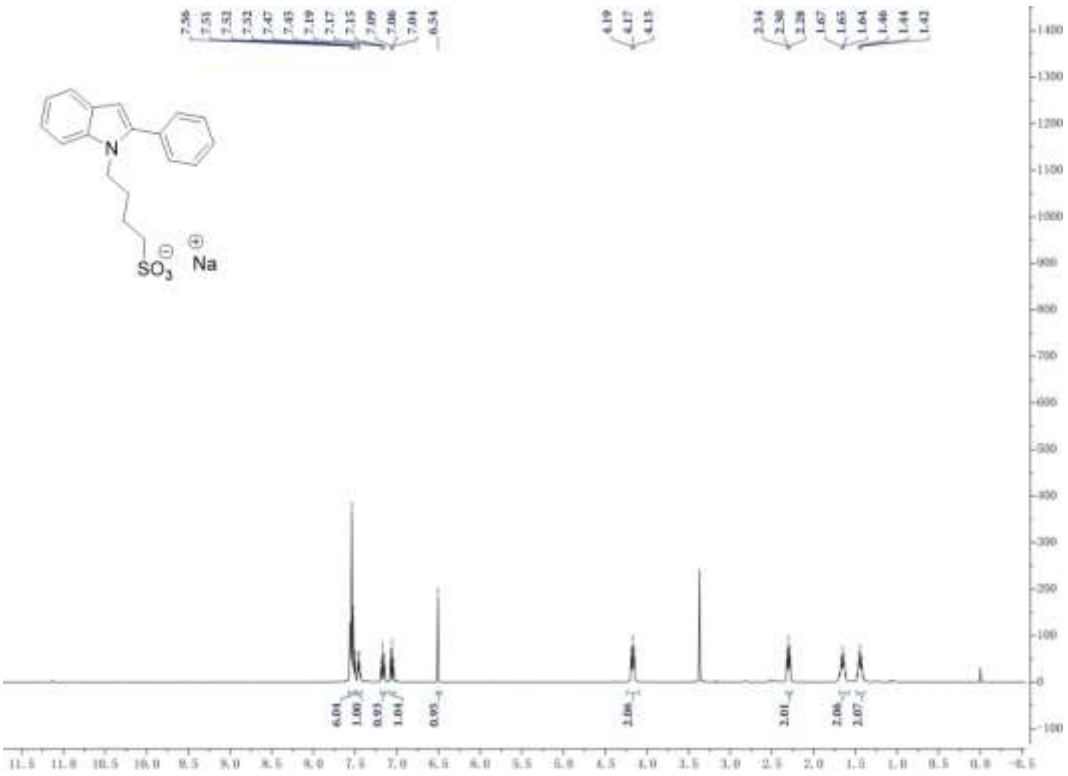

Figure S36. The ^{1}H-NMR spectrum of **Compound 4** in DMSO-d_6.

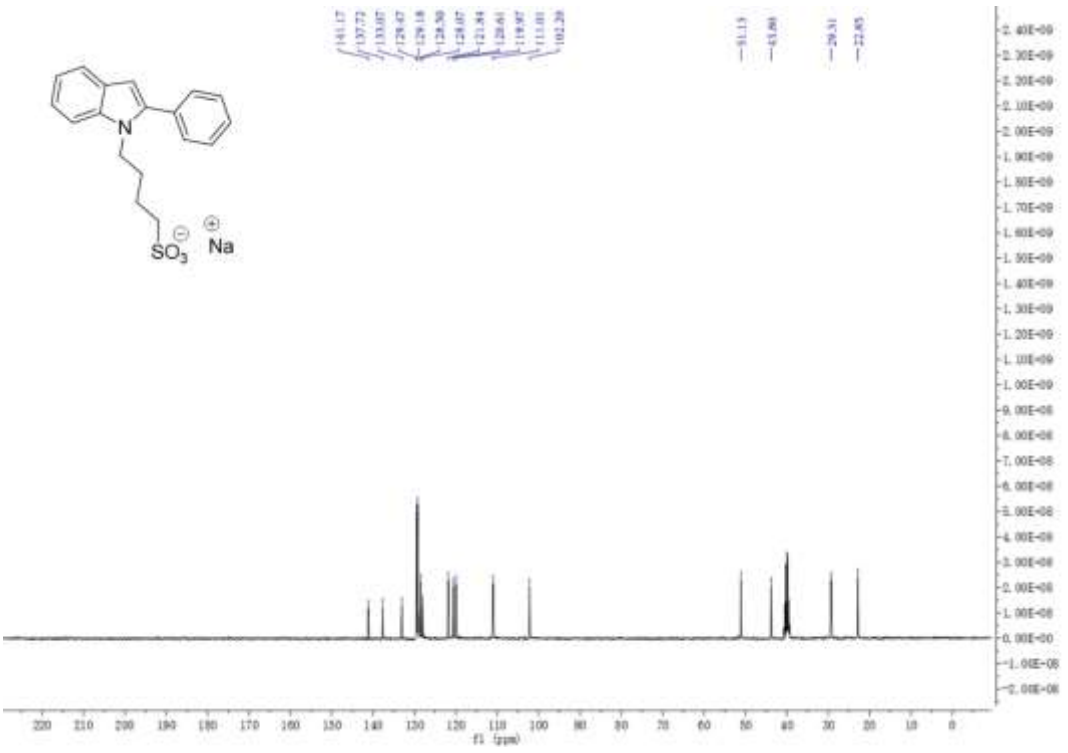

Figure S37. The ^{13}C-NMR spectrum of **Compound 4** in DMSO-d_6.

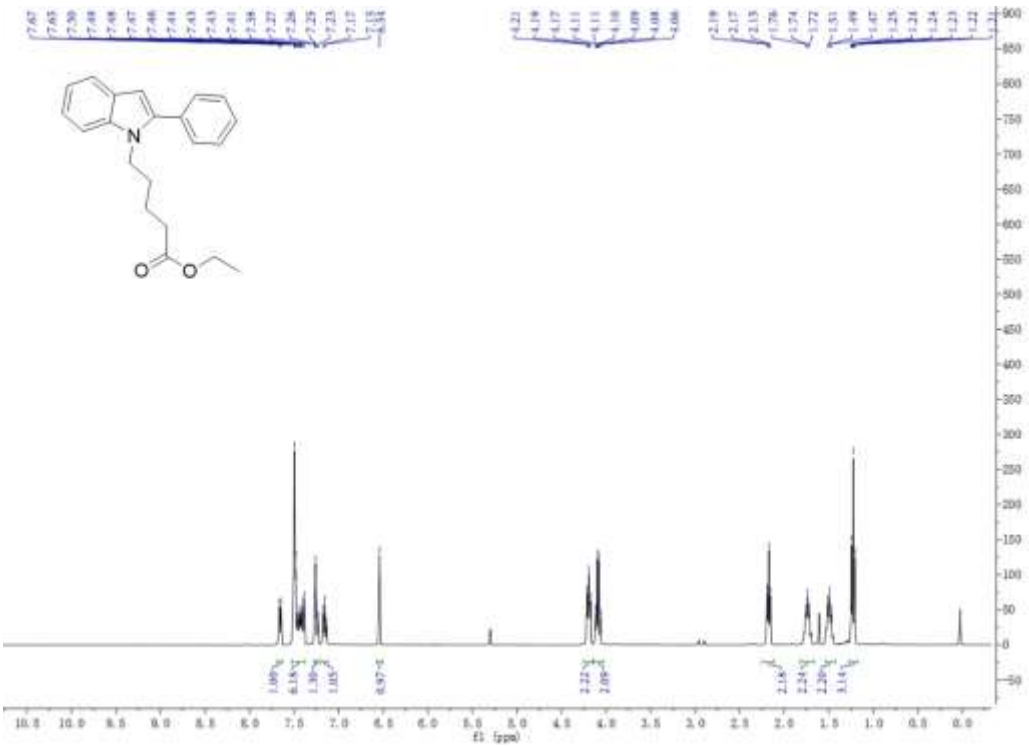

Figure S38. The ^{1}H-NMR spectrum of **Compound 5** in $CDCl_3$.

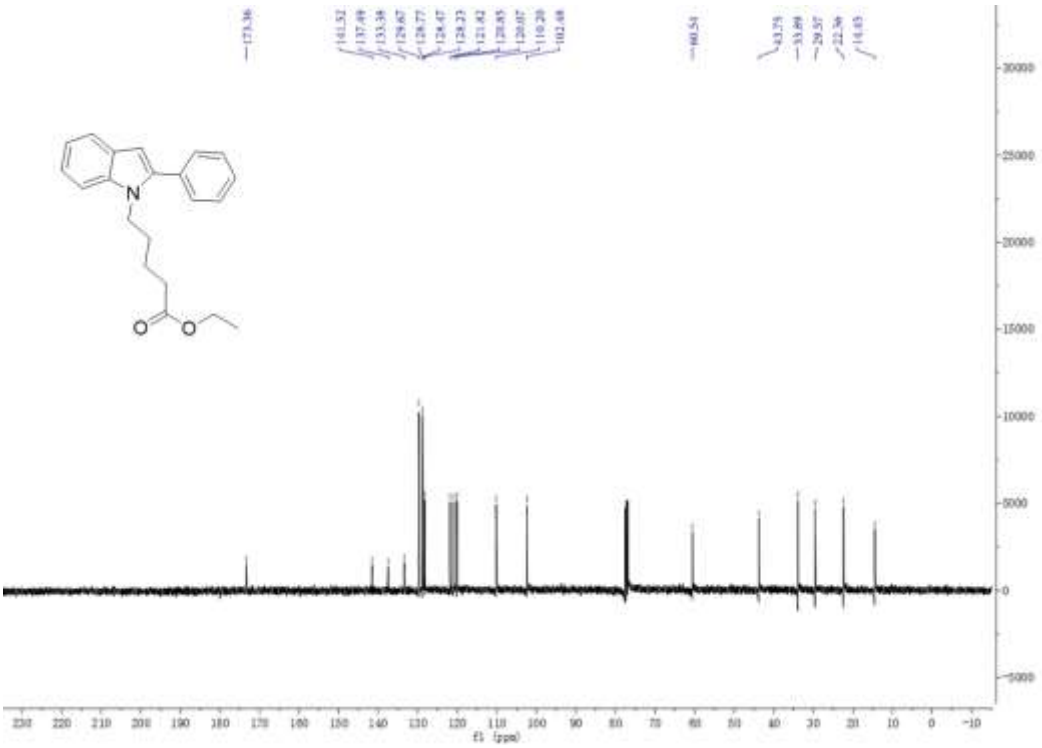

Figure S39. The ^{13}C-NMR spectrum of **Compound 5** in $CDCl_3$.

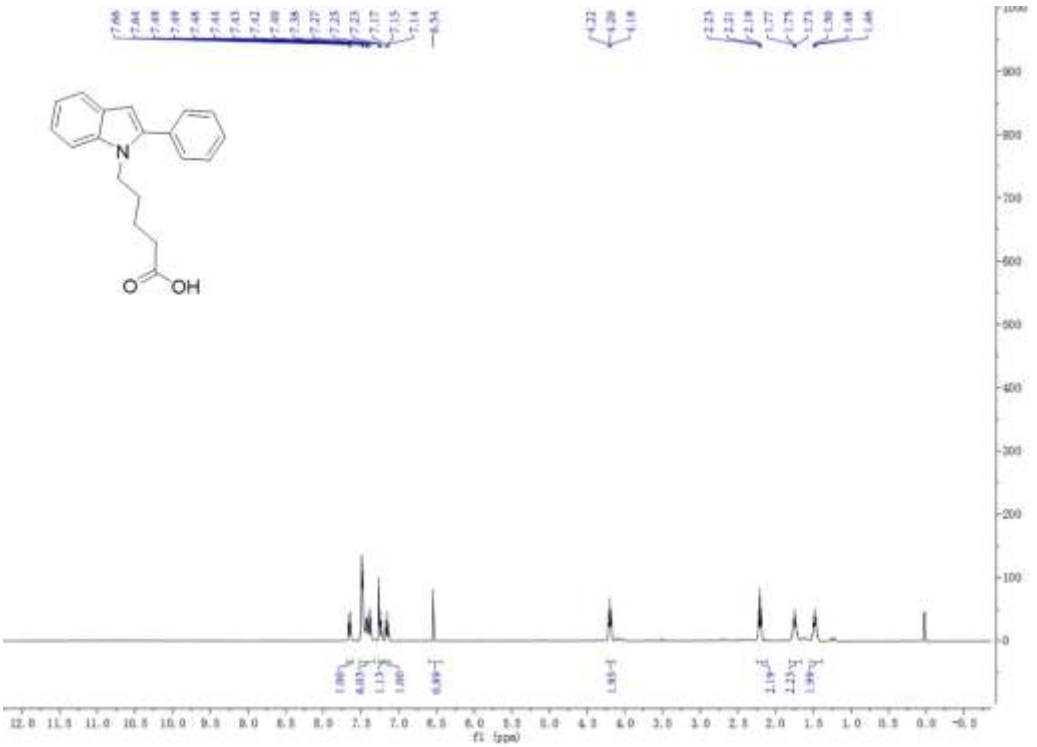

Figure S40. The ^{1}H-NMR spectrum of **Compound 6** in $CDCl_3$.

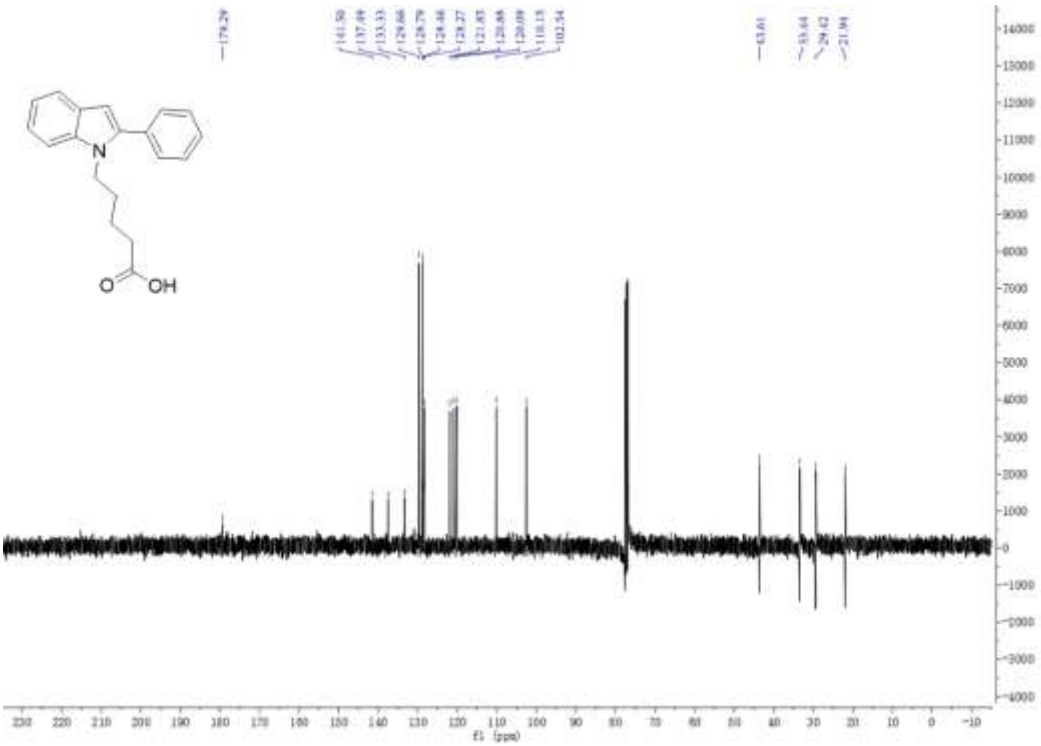

Figure S41. The ^{13}C-NMR spectrum of **Compound 6** in $CDCl_3$.

References

[1] F. Wang, R. Deng, X. Liu, *Nat Protoc.* **2014**, *9*, 1634.

[2]. Liang. Y. Lu, R. Zhang, A. C. Tiago, A. O. Sergey, M. Deyevde, Y. Qian, A. V. Zvyagin, *Acta Biomater.* **2017**, *51*, 461.

[3] X. Ai, Z. Wang, H. Cheong, Y. Wang, R. Zhang, J. Lin, Y. Zheng, M. Gao, B. Xing, *Nat. Commun.* **2019**, *10*, 1087.

[4] A. Sedlmeier, H. Gorris, *Chem. Soc. Rev.* **2015**, *44*, 1526.

[5] Y. Fan, P. Wang, Y. Lu, R. Wang, L. Zhou, X. Zheng, X. Li, J. A. Piper, F. Zhang, *Nat. Nanotechnol* **2018**, *13*, 941.

[6] T. Peng, N. Wong, X. Chen, Y. Chan, D. H. H. Ho, Z. Sun, J. J. Hu, J. Shen, H. El-Nezami, D. Yang, *J. Am. Chem. Soc.* **2014**, *136*, 11728.